3. SITE 566[1]

Shipboard Scientific Party[2]

HOLE 566

Date occupied: 24 January 1982, 0040 hr.

Date departed: 25 January 1982, 1215 hr.

Time on hole: 35 hr., 35 min.

Position: 12°48.34′N; 90°41.79′W

Water depth (sea level; corrected m, echo-sounding): 3745

Water depth (rig floor; corrected m, echo-sounding): 3755

Bottom felt (m, drill pipe): 3786

Penetration (m): 55.8

Number of cores: 9

Total length of cored section (m): 55.8

Total core recovered (m): 21.46

Core recovery (%): 38.4

Oldest sediment cored:
  Depth sub-bottom (m): 21.9
  Nature: dark olive gray mudstone
  Age: late Pleistocene
  Measured velocity (km/s): 1.589

Basement:
  Depth sub-bottom (m): 29
  Nature: serpentinized peridotite
  Velocity range (km/s): 3.901

HOLE 566A

Date occupied: 25 January 1982, 1500 hr.

Date departed: 25 January 1982, 1715 hr.

Time on hole: 2 hr., 15 min.

Position: 12°47.91′N; 90°41.99′W

Water depth (sea level; corrected m, echo-sounding): 3826

Water depth (rig floor; corrected m, echo-sounding): 3836

Bottom felt (m, drill pipe): 3865

Penetration (m): 7

Number of cores: 1

Total length of cored section (m): 7

Total core recovered (m): 0.12

Core recovery (%): 1.7

Oldest sediment cored: none recovered

Basement:
  Depth sub-bottom (m): 6
  Nature: serpentinized peridotite
  Velocity range (km/s): 4.485

HOLE 566B

Date occupied: 25 January 1982, 2015 hr.

Date departed: 26 January 1982, 0150 hr.

Time on hole: 5 hr., 35 min.

Position: 12°48.81′N; 90°41.50′W

Water depth (sea level; corrected m, echo-sounding): 3661

Water depth (rig floor; corrected m, echo-sounding): 3671

Bottom felt (m, drill pipe): 3674

Penetration (m): 49

Number of cores: none

Total length of cored section (m): none

Total core recovered (m): none

Core recovery (%): none

HOLE 566C

Date occupied: 26 January 1982, 1100 hr.

Date departed: 29 January 1982, 0420 hr.

Time on hole: 65 hr., 20 min.

Position: 12°48.84′N; 90°41.53′W

Water depth (sea level; corrected m, echo-sounding): 3661

Water depth (rig floor; corrected m, echo-sounding): 3671

Bottom felt (m, drill pipe): 3673

Penetration (m): 136.6

Number of cores: 7

Total length of cored section (m): 65.8

Total core recovered (m): 5.82

Core recovery (%): 8.8

Oldest sediment cored:
  Depth sub-bottom (m): 88.1
  Nature: mudstone and santstone
  Age: late Miocene
  Measured velocity (km/s): 2.871

Basement:
  Depth sub-bottom (m): 109.1
  Nature: serpentinized peridotite
  Velocity range (km/s): 3.990–4.184

Principal results (Holes 566–566C): The main result at Site 566 was certainly the unexpected discovery of serpentinite and serpentinized peridotite under the slope deposits at the bottom of three holes. This occurrence is yet another one along Central America and suggests a comparison with the peridotites cropping out in Central America.

The fact that late Miocene or late Pleistocene sediment rests directly on the peridotite confirms the position of Site 566 in a canyon zone, as was suspected before drilling.

The gas present in the serpentinized peridotites at Hole 566C has certainly migrated, probably along a soft zone of easily drilled sheared serpentine encountered between sub-bottom depths of 117 and 126 m.

BACKGROUND AND OBJECTIVES

Site 566 is about two-thirds of the way down the Middle America Trench slope, in 3700 m of water, 2300 m above and 22 km landward from the Trench axis. It is in the lower reaches of San José Canyon and was selected because of the thin slope deposits over acoustic basement.

Multichannel seismic record GUA-2 shows an irregular, thin cover of slope deposits on the relatively smooth lower slope of the Trench. Acoustic basement is here without internal reflections, in contrast to the landward-dipping reflection beneath the upper slope. At about 5 km depth is a reflective sequence dipping gently landward that can be traced from the Trench at least 25 km under the continental slope. This reflective sequence marks oceanic crust subducted beneath the Middle American margin.

Two major objectives at Site 566 were: (1) to recover the slope deposits in order to know their age, the history of the margin during the time of sedimentation (uplifting and/or subsidence), and the nature of the contact at the base of the slope deposits; (2) to penetrate the acoustic basement in order to discover its age and facies, and to compare these with the sequences recovered at Site 494 during Leg 67; from such information we hoped to learn more about tectonic history and the tectonic mechanisms that formed this margin.

OPERATIONS

Glomar Challenger left the rendezvous with the Costa Rican Coast Guard off Cabo Blanco at 1230L (local time), 19 January and steamed to Site 566 with all geophysical gear operating in the normal under-way mode. At 2300L, 20 January, as we were entering Guatemalan waters, we retrieved seismic gear, and shortly thereafter the *Glomar Challenger* was at the site, using only a depth sounder. While waiting for permission from the Guatemalan government to drill, *Glomar Challenger* did a survey around the site, using its echo sounder to better map the lower part of San José Canyon.

On 21 January, 1830L, we received an order to proceed to a new site in international waters located at 7°03.2′N; 91°42.5′W. *Glomar Challenger* departed immediately with only its echo sounders operating until out of Guatemalan waters.

On 22 January, 1635L, we were informed that the government of Guatemala had granted official written permission for drilling at all the sites on the Guatemala margin. *Glomar Challenger* came back immediately with all gear in for complete profiling.

On 23 January at 2202L, a beacon was dropped at Site 566. The position was 12°48.34′N; 90°41.79′W. After completing a short survey around the site, *Glomar Challenger* returned to the beacon. At 0040L, 24 January, we began to run pipe in the hole.

The first core was recovered at 1700L, 24 January. Because of the stiffness of the mud, the HPC (hydraulic piston core) was only used for the first two cores, then we switched to rotary coring, using a new extended core barrel. Core 9 came up at 1207L, 25 January with the same serpentinite as recovered in all cores since 5; we decided to study the extent of this serpentinized peridotite body.

From 1215 to 1500L, 25 January, the bit was pulled above the seafloor, and *Glomar Challenger* made an offset of 3000 ft. from the beacon on bearing 206°, to the new Hole 566A, located at 12°47.91′N, 90°41.99′W. Drilling began at 1500L, coring through 6 m of sediment and then 1 m of serpentinized peridotite. Because of the lack of a sufficient sedimentary cover, we abandoned the hole and pulled the bit above the seafloor at 1715L.

From 1715 to 2015L, 25 January, *Glomar Challenger* made an offset of 3000 ft. from the beacon on bearing 026°, to Hole 566B, located at 12°48.81′N, 90°41.50′W. Drilling began at 2015L, washing out the first 49 m of sediments, and then coring. On 26 January, 0150L, the first core came up with no recovery because of obvious problems with the XCB (extended core barrel) system. We decided to trip the drilling string for a new bottom-hole assembly.

After washing out 49.8 m of sediment, the first core was recovered at 0145L 27 January, from Hole 566C, located essentially at Hole 566B (12°48.84′N; 90°41.53′W). Four cores were recovered in sediment. Then the drilling proceeded by washing out to the basement, which was reached at a depth of 109.1 m, where three cores containing serpentinized peridotites were recovered, Core 7 coming up at 1834L 27 January. The bit was continually plugged, and so we decided to stop the drilling and prepare for logging. Circulation was regained at 2130L, the bit released at 2245L, and the hole was filled with 12-lb., bentonite barite mud for logging.

Logging began at 0400L with a sonic, natural gamma, and caliper tool, but an impenetrable bridge had formed at 65 m below the seafloor. When the tool was retrieved, the drill pipe was pushed through the bridge, and we decided to run another log. After rigging and running down, it was impossible to get out of the pipe, and so the hole was abandoned. The *Challenger* left the site at about 2200L, crossing the beacon for a position enroute to Site 567.

Table 1 shows the coring summary for this site.

LITHOSTRATIGRAPHY AND IGNEOUS PETROLOGY

Introduction

Site 566 is located on the top of the lower slope of the Middle America Trench, about 25 km northeast of the Trench axis and 100 km south of the Guatemalan coast (Fig. 1). Four holes, 566, 566A, 566B, and 566C, were

Table 1. Coring summary, Site 566.

Core	Date (Jan., 1982)	Time	Depth from drill floor (m) Top Bottom	Depth from seafloor (m) Top Bottom	Length cored (m)	Length recovered (m)	Recovery (%)
Hole 566							
1	24	1700	3786.0–3790.0	0.0–4.0	4.0	3.70	93
2	24	1820	3790.0–3796.0	4.0–10.0	6.0	5.96	99
3	24	2119	3796.0–3798.3	10.0–12.3	2.3	Trace	0
4	24	2249	3798.0–3807.9	12.3–21.9	9.6	4.65	48
5	25	0053	3807.9–3817.4	21.9–31.4	9.5	3.95	42
6	25	0310	3817.4–3827.1	31.4–41.1	9.7	1.26	13
7	25	0550	3827.1–3836.8	41.1–50.8	9.7	0.60	6
8	25	0912	3036.8–3838.8	50.8–52.8	2.0	0.64	32
9	25	1207	3838.8–3841.8	52.8–55.8	3.0	0.70	23
Total					55.8	21.46	38
Hole 566A							
1	25	1641	3865.0–3872.0	0.0–7.0	7.0	0.12	2
Total					7.0	0.12	2
Hole 566B							
H1	26	Washed	3673.0–3723.0	0.0–49.0	—	—	—
Hole 566C							
H1	26	Washed	3675.0–3724.8	0.0–49.8	—	—	—
1	27	0145	3724.8–3734.3	49.8–59.3	9.5	0.00	0
2	27	0318	3734.3–3743.8	59.3–68.8	9.5	0.86	9
3	27	0455	3743.8–3753.5	68.8–78.5	9.7	0.13	1
4	27	0610	3753.5–3763.1	78.5–88.1	9.6	0.00	0
H2	27	Washed	3763.1–3784.1	88.1–109.1	—	—	—
5	27	1220	3784.1–3792.2	109.1–117.2	8.1	1.73	21
6	27	1525	3792.2–3801.9	117.2–126.9	9.7	1.34	14
7	27	1834	3801.9–3811.6	126.9–136.6	9.7	1.76	18
Total					65.8	5.82	9

Note: — indicates no cores recovered.

drilled in order to determine the lithology of the acoustic basement and the age of the oldest slope deposits (overlying this basement). The lithostratigraphy and sedimentology of the three holes from which material was recovered (566, 566A, and 566C) are described individually as follows.

Hole 566

Hole 566 was drilled 3786 m below sea level and was cored continuously to a depth of 56 m. Recovery was excellent down to 26 m sub-bottom, where igneous basement material was first encountered. Three units are distinguished (Fig. 2). The contact between Units I and II is gradational over 0.5 m (Core 5). The contact between Unit II and Basement was not recovered but is probably sharp.

Unit I

Unit I comprises Cores 1 to 5, 0 to 26 m sub-bottom depth; (late Pleistocene).

Major lithology. This unit is a relatively uniform late Pleistocene section of generally dark olive gray (5Y 3/2) siliceous mud.

Sedimentary structures are quite common in the upper part of the hole (Cores 1 and 2), composed of finely laminated silty beds, which are commonly normally graded, and a few isolated silty beds. Small subrounded to subangular pebbles of mudstone are uncommon but are found dispersed throughout the section, notably in Cores 1 and 5. Pyrite and serpentinite pebbles are quite common in Core 5. Mottling of the mud present in Cores 1, 2, and 5 results from bioturbation. Bioturbation is observed in Cores 2, 4, and 5.

The average sand–silt–clay percentages based on shipboard smear-slide analyses for this unit are 5, 40, and 55%, respectively. The major detrital component is clay, although minor amounts of quartz, plagioclase feldspar, and other terrigenous material are present. Glauconite is found in quantities less than 3%.

Well-preserved diatoms, radiolarians, and sponge spicules account for up to 15% of the composition of the mud. Foraminifers are quite rare and of mediocre preservation. Much of the unspecified carbonate detritus (in concentrations of up to 10% of the total sediment in most samples) may be broken foraminifer tests.

Several postdepositional structures were observed, most commonly, microfracturing of the massive mud. Although most of this fracturing was probably caused by drilling disturbances, the consensus among most of the shipboard party was that some of the fractures occurred *in situ*. Small faults are common (Core 2), and calcium
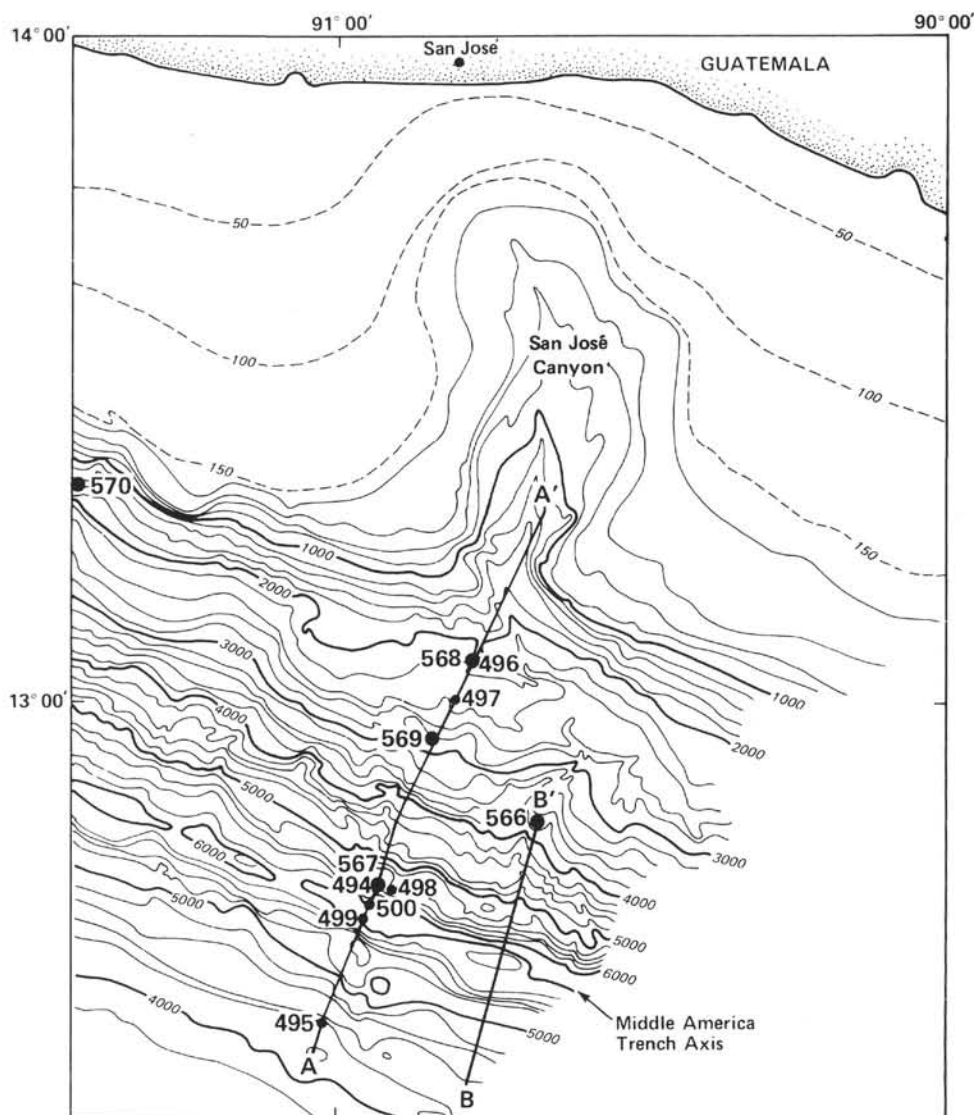
Figure 1. Bathymetric map of the Guatemala margin and San José Canyon, showing the UTMSI seismic record GUA-13 (A–A′), the location of Legs 67 and 84 sites off Guatemala, and the area of Figure 10 (B–B′).

carbonate was precipitated along one of these faults. A postdepositional penetrative fabric, best described as a "scaliness," was observed interbedded with the massive mud near the top of Core 2. As at Site 565, we believe that this scaliness may be a feature of primary deformation such as slumping.

Minor lithology. Fine-grained, sandy mud (5Y 3/2, dark olive gray) is occasionally interbedded with the major lithology throughout Unit I (see Cores 1 and 2) in beds up to 2 cm thick.

Sedimentary structures are quite rare but include grading and parallel laminations. The sand beds are sometimes erosive; one bed in Core 2 showed a good scour and fill structure. Loading and injection of sand into the underlying mud was also observed. An apparent dip of 20° was recorded throughout Unit I.

The composition of the sandy mud is predominantly subrounded to subangular grains of quartz and feldspar, although a lot of carbonate detritus is present (up to 20%). Siliceous microfossils are rare within the sands.

Unit II

Unit II comprises Core 5, 26 to 29 m sub-bottom depth (late Pleistocene).

Major lithology. This is a late Pleistocene matrix-supported breccia. The matrix is dark olive gray (5Y 3/2) and the clasts are black (7.5YR 3.5/2).

No internal sedimentary structures are found within this unit. Angular clasts of serpentinite and tuff up to 3 cm in diameter are supported by a matrix of calcareous–dolomitic mud (see Diagenesis section) that is variably cemented. An increase in clast size is observed from the top to the base of this unit. Very little fossiliferous material is seen in the matrix.

A postdepositional scaly fabric is present in the mud matrix, perhaps from sediment or mass movement.

Basement

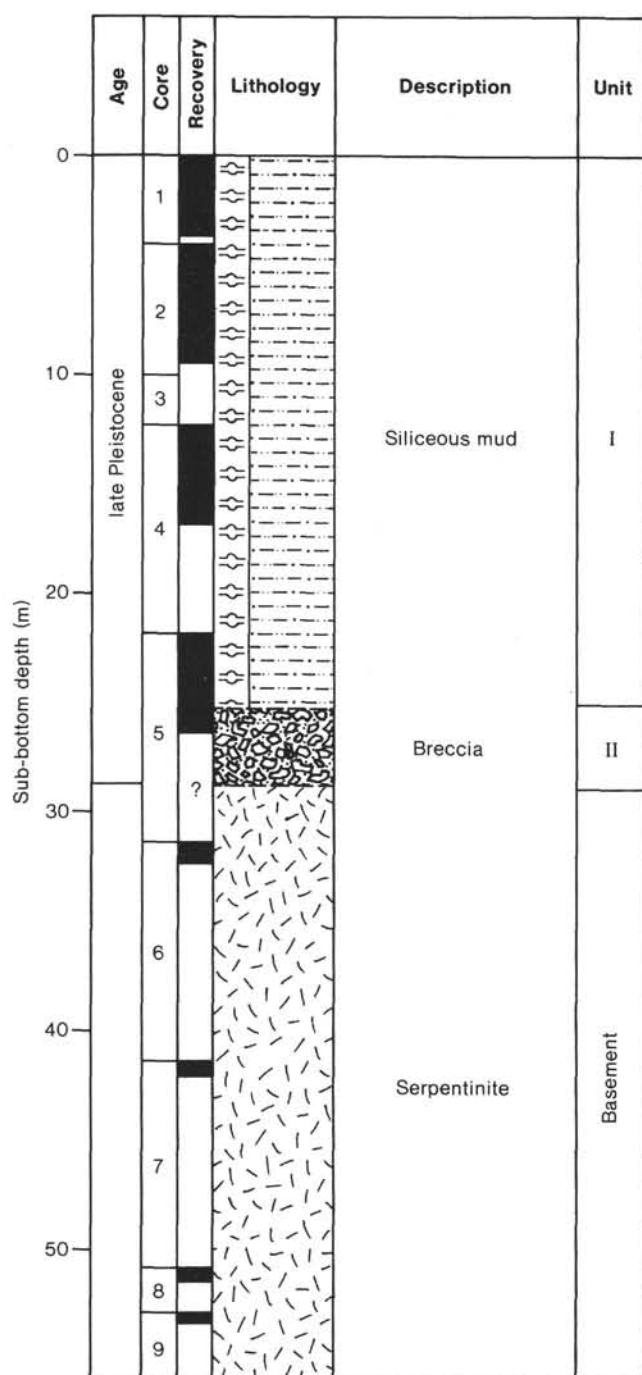Basement ranges from Cores 6 to 9, 29 to 56 m sub-bottom (age unknown).

Figure 2. Lithostratigraphic summary of Hole 566.

Major lithology. The basement comprises a serpentinite that commonly displays internal shearing. A full description of the serpentinite is included in the Igneous Petrology section.

Hole 566A

Hole 566A was drilled 3865 m below sea level and was cored continuously to a depth of 7 m where basement was encountered. Recovery was very poor—only a few rock fragments were recovered from the core catcher. From these fragments two main lithologic units could

be distinguished (Fig. 3). No contact between the units was recovered.

Unit I

Unit I, less than 6 m sub-bottom (late Pliocene), comprises a dark greenish gray siliceous mud (5GY 4/5). It is massive and possesses no internal sedimentary structures. The sand–silt–clay percentages of this unit are 10%, 20%, and 70%, respectively (based on shipboard smear-slide analyses). The major detrital component is clay, although minor sand-sized grains of quartz, feldspar, and mica are present. Siliceous microfossils account for up to 10% of the mud. Carbonate detritus accounts for up to 15% of the mud. Some traces of authigenic pyrite were observed.

Basement

Basement (6 m sub-bottom; age unknown) comprises serpentinite similar to that recovered from Hole 566 basement. A full description is included in the Igneous Petrology section.

Hole 566C

Hole 556C was drilled 3675 m below sea level after we abandoned Hole 566B without recovering sediment. Two wash cores were taken after washing down from 0 to 49 m sub-bottom and from 88 to 109 m sub-bottom, respectively. The remainder of the hole to 136 m subbottom was cored continuously. Recovery was very poor, and any lithostratigraphic column must be interpreted with caution (Fig. 4). Well logging of Hole 566C may help determine the stratigraphy more precisely (see Physical Properties section). For the purposes of this site report, the stratigraphy is divided into three units. No contacts between units were recovered.

Unit I

Unit I comprises 0 to about 50 m sub-bottom depth (Pleistocene to late Miocene).

Major lithology. This unit comprises a dark olive gray (5Y 5/2) Pleistocene to late Miocene mud. Drilling disturbance accounts for the absence of any sedimentary structures. The average sand–silt–clay percentages for this unit are 20, 30, and 50%, respectively (based on shipboard smear-slide analyses). Clay is the major detri-
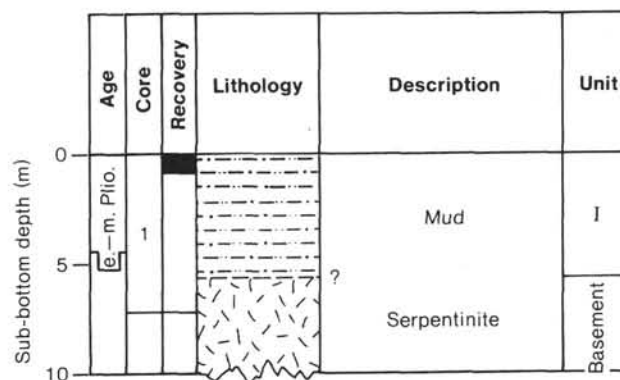

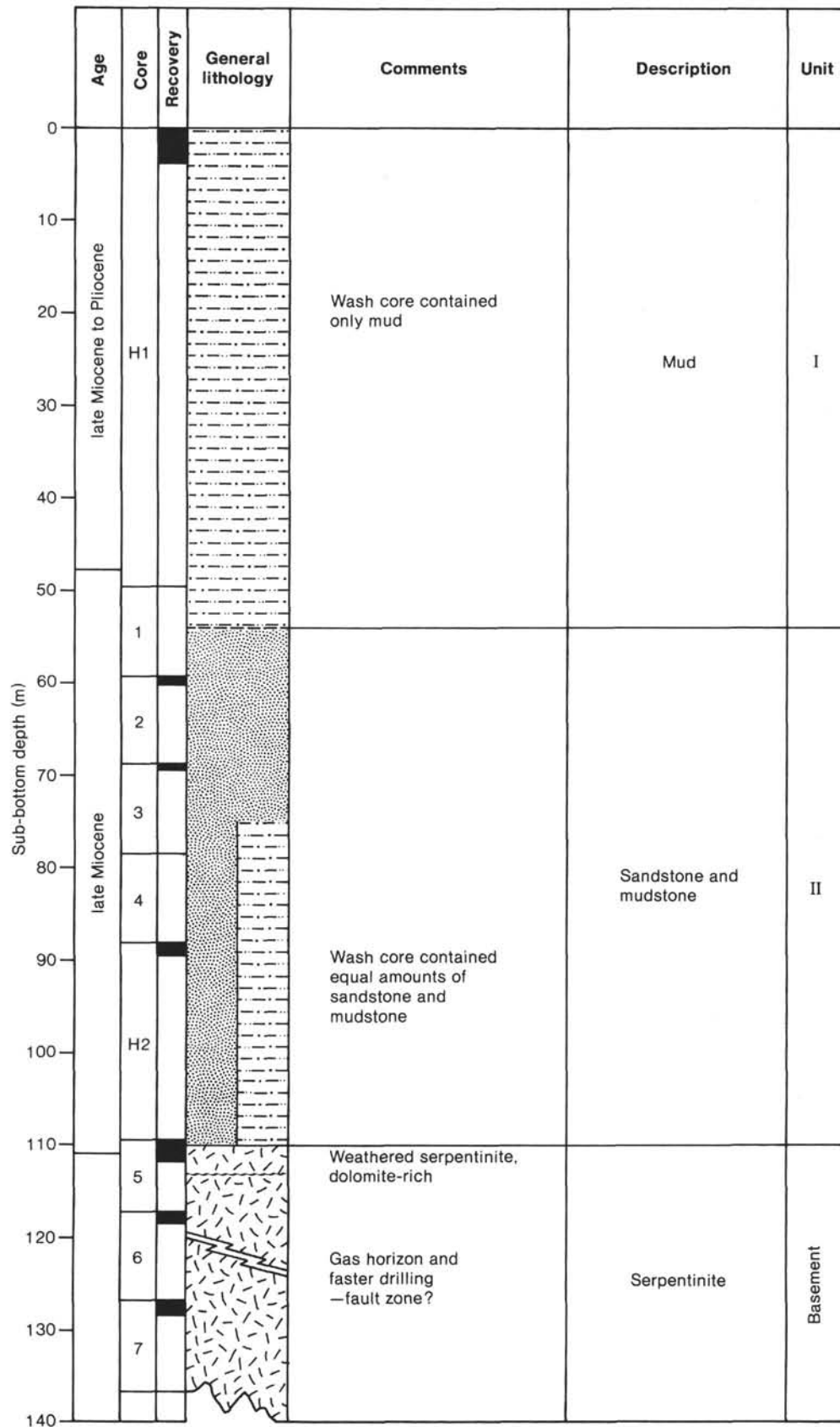Figure 3. Lithostratigraphic summary of Hole 566A.

Figure 4. Lithostratigraphic summary of Hole 566C.

tal component, although substantial amounts of quartz (up to 30%) and feldspar are present.

Unit II

In Unit II (50 to 110 m sub-bottom depth; late Miocene), recovery was very poor and included a wash core mixture from 88 to 110 m, so detailed treatment of the sedimentology is fairly subjective. Equal amounts of sandstone and mudstone fragments were recovered from the drilling breccias. The mudstone is dark olive gray (5Y 3/2), and the sandstone olive gray (5Y 4/2) to dark greenish gray (5Y 4/1).

Basement

Basement (Cores 5 to 7, 110 to 137 m sub-bottom; age unknown) contains a serpentinite that commonly displays shearing. A full description of the serpentinite is included n the Igneous Petrology section. The top 2 to 3 m of the serpentinite is weathered to a clayey texture, but internal structures are preserved. There may be a tectonic contact within Core 6, given that highly sheared serpentinite was recovered. The tectonic contact may also explain the increased drilling rates in the same region as well as the presence of gas (see Geochemistry section).

Igneous Petrology

At the base of Holes 566, 566A, and 566C, serpentinite basement was recovered. In Holes 566 and 566C the upper contact of the serpentinite is greatly altered, with serpentine and possibly brucite being replaced by dolomite and a mineral from the pyroaurite–hydrotalcite group. The ultramafic rocks of Holes 566, 566A, and 566C can be divided into three categories:

1. Serpentinite containing about 20% unaltered mineral assemblage. The predominant original mineral present is forsteritic olivine, although enstatitic orthopyroxene (partially replaced by serpentine pseudomorphs) is also present. The orthopyroxenes exhibit pyroclastic textures. Diopsidic clinopyroxenes are commonly found at exsolution laminae in the orthopyroxenes. Brown red chromite spinel is abundant. The major alteration product of the original igneous rock is serpentinite. The serpentine exhibits mesh structures enclosing olivine and also occurs as serpentine ribbon textures with no original minerals.

2. Serpentinite containing almost no original minerals. This rock shows a complete alteration to serpentinite that has a ribbon texture. Magnetite is scattered throughout the groundmass, forming an augen texture with the foliated serpentine. Some of this magnetite seems to be an alteration product of chromite. Chrysotile is found within crosscutting veins in the sheared fabric of the serpentinite.

3. Weathered serpentinite. The weathered serpentinite is a replacement product of both serpentinite types just described. The replacement minerals are dolomite and an unidentified member of the pyroaurite-hydrotalcite group (identification by shipboard XRD—X-ray diffraction). Serpentinite is replaced in places by rhom-

bohedric dolomite crystals. Dolomite veins also crosscut the rock.

The structure and mineralogy of the ultramafic mineral assemblage of the serpentinite suggests that the original rock type was peridotite. The predominance of serpentine over brucite also suggests that the olivine/orthopyroxene ratio was "harzburgitic." The mineral assemblage (talc, serpentine, and magnetite) of the serpentinite indicates a very low alteration temperature (probably below 300°C). The dominant foliation that occurs in the completely replaced serpentinite indicates that there was some shear stress during alteration.

Summary of Lithostratigraphy

Canyon Deposits and Processes

Site 566 was drilled within a submarine canyon, so examination of the sedimentary facies encountered provides valuable information regarding processes operating within canyons.

Observations of the physical properties show that in Cores 566-1 and 566-2, less than 10 m sub-bottom depth, the sediment is firmer than would be expected from normal overburden pressures (see Physical Properties). This factor is reflected in the style of early deformation structures that include fracturing (i.e., brittle failure). Overconsolidation could have resulted from an earlier, greater pile of sediment that has since been removed by mass flow or processes operating within the canyon.

Four main sedimentary facies were encountered at Site 566:

1. Pebbly mud (Core 5): mass movement or slumping
2. Massive mud (Core 4): mass movement or slumping
3. Graded sandstone beds (Cores 1 and 2): current activity
4. Laminated muds (Cores 1 and 2): current activity.

Facies 3 and 4 can be attributed to deposition by current activity. In the case of facies 3 there is no doubt that the sand was deposited from a turbidity current. Facies 1 and 2 were probably deposited from debris flows. Thus the canyon deposits of Site 566 are dominated by mass flow deposits and "turbidites."

A complex pattern of erosion and deposition can be inferred from the different ages of slope deposits in contact with the basement. At Hole 566 only Pleistocene mud was recovered, at Hole 566A Pliocene mud was recovered, and at Hole 566C late Miocene mud overlies the basement. Sandstone petrography, geophysical surveys, bathymetric profiles, and conventional oceanographic dredging samples (Ladd et al., 1978) also demonstrate that basement is exposed in the canyon. This basement exposure suggests either long periods of nondeposition or, more likely, periodic erosion of sediment.

A higher percentage of sandstone was recovered from Holes 566, 566A, and 566C than at Site 565 or the Leg 67 sites that were drilled in between canyons, suggesting

that coarser sediment tends to be constrained to canyons during downslope transportation.

Basement Topography

Drilling at Site 566 confirmed that the slope deposits/basement contact seen in geophysical records has considerable relief. This fact may indicate that earlier structures have been eroded. Breccias and present exposure of basement to submarine sedimentary and weathering processes indicate that erosion took place in the San José Canyon at least as early as the late Miocene and is still occurring today.

Basement Composition

The composition of the basement at Site 566 is serpentinite, which may represent the submarine extension of similar serpentinite occurrences found on the Middle America continental framework.

Sedimentary Provenance

The sediment at Site 566 was derived from the Tertiary and Quaternary volcanic rocks exposed in Guatemala. Reworked Cretaceous nannofossils and Cenozoic benthic foraminifers may have been derived from sediment exposed upslope (see Biostratigraphy section).

BIOSTRATIGRAPHY

Introduction

Pleistocene to Miocene microfossils were recovered from the mudstones and muddy sandstones drilled in three of the four holes at Site 566. Calcareous nannofossils occur in moderately preserved, low to common abundances, whereas diatoms are once again present in low numbers typical of heavy terrigenous admixture. Benthic foraminifers also occur in low numbers, are moderately preserved, and offer limited data from which to determine the paleoecology. Hole 566 contains 22 m of Pleistocene mudstones on serpentinite basement; Hole 566A contains 7 m of Pliocene (probably late) mudstone; and Hole 566C contains approximately 38 m of late Miocene muddy sandstone. No datable sediment was recovered from Hole 566B. Rare reworked Cretaceous nannofossils are present in both Holes 566 and 566C. All paleontologic disciplines are in general age agreement and are summarized in Figure 5.

Sediment accumulation rates uncorrected for compaction (Fig. 6) are approximately 75 m/m.y. for all three holes. This figure seems anomalously high for a canyon area that has undergone erosion since at least the late Miocene. The period of time represented by the recovered sediments is near the limits of paleontological resolution (0.5 m.y. or less), which suggests that accumulation rates are uncertain.

Ecologic analysis of benthic foraminifers indicates that deposition occurred at lower bathyal to abyssal depths and that downslope transport was derived primarily from the upper and middle slope regions. During the late Miocene–early Pliocene a fine sand was deposited at abyssal depths (≤4000 m). Foraminiferal specimens were transported from the upper and middle slopes, probably as sand grains, because these specimens are poorly preserved, rare, and size sorted. Assemblages in Hole 566 suggest shallowing of the area during the Pleistocene to the lower bathyal biofacies (2000–4000 m). Transported specimens are principally from the low oxygen zone of the upper slope (approximately 1200–1500 m). These transported faunas dominate the assemblages, have low diversities, and are size sorted.

Calcareous Nannofossils

Pleistocene to late Miocene sediments (summarized in Fig. 5) were recovered on shallow serpentinite basement at all but Hole 566B, which had no core recovery. Late Pleistocene nannofossils are abundant and well preserved. Slight dissolution of placoliths resulted in the destruction of the central bar in occasional specimens of *Gephyrocapsa*. Pliocene nannofossils occur in lesser numbers with similar, slightly etched preservation, whereas late Miocene nannofossil assemblages occur in very low, poorly preserved numbers with overgrowth of *Discoaster* species, fragmentation of *Ceratolith* species, and etching of placolith species — indicating significant diagenesis and possible downslope transport.

Reworking of nannofossils is sparse and restricted primarily to Cretaceous species at Holes 566 and 566C. *Sphenolithus neoabies* (middle Miocene-early Pliocene) occurs in 556A-1,CC in an unusually low abundance, which indicates that its presence is also the result of reworking into a late Pliocene sample.

Hole 566

Section 566-1-2 through Sample 566-5-2, 83 cm are assigned to the late Pleistocene–Recent *Emiliania huxleyi–Pseudoemiliania lacunosa* Zones. Abundant, minute placoliths with affinities to *E. huxleyi* were observed in 566-1,CC, with small *Gephyrocapsa* spp., *Crenalithus* spp., *Helicosphaera kamptneri*, and *Gephyrocapsa oceanica*. Samples 566-2,CC through 566-4,CC continue to be dominated by this assemblage without the presence of *E.* cf. *huxleyi*. Sample 566-3,CC also contains very rare *Nannoconus* sp. reworked from the Cretaceous. Very rare *Pseudoemiliania lacunosa* (less than 0.01% of the total assemblage) are reworked in 566-4,CC. Samples 566-5,CC through 566-9,CC contain serpentinite and are of course barren of nannofossils.

Hole 566A

Hole 566A recovered only one core, which contained mudstone mixed with serpentinite in 566-1,CC. The age of the marine mudstone in this sample is probably late Pliocene, with a flora dominated by *Crenalithus* spp., *Helicosphaera kamptneri, Discoaster brouweri, Calcidiscus macintyrei*, and very rare *Discoaster pentaradiatus*. The co-occurrence of these species is indicative of the *Discoaster brouweri* Zone. Very rare specimens of *Sphenolithus neoabies*, which is ubiquitous throughout the early Pliocene and late Miocene, are thought to be reworked, because they make up less than 0.01% of the assemblage; no other early Pliocene species are present.

Core				Age	Biostratigraphy			Paleo-bathymetry				
Hole 566	Hole 566A	Hole 566B	Hole 566C		Nannofossil zones	Diatom zones	Benthic foraminifers	Neritic	Bathyal			Abyssal
									Upper	Middle	Lower	
1				Pleistocene	Emiliania huxleyi– Pseudoemiliania lacunosa	Pseudoeunotia doliolus	Pleistocene					
2												
3						Nitzschia reinholdii						
4												
5					/////	/////						
6												
7												
8												
9												
	1			late Pliocene	Discoaster brouweri	Pliocene	late Tertiary					
		None			No recovery	No recovery	No recovery					
			H1	late Miocene	Discoaster quinqueramus	Pliocene to late Miocene	Pliocene					
			1									
			2				late Miocene					
			3			/////						
			4				No recovery					
			H2				late Miocene					
			5		/////							
			6									
			7									

Figure 5. Biostratigraphic and paleoecologic summary, Holes 566, 566A, 566B, and 566C. Hachures indicate barren intervals.

Holes 566B and 566C

Hole 566B was washed to 49.0 m, and no sediments were recovered.

Hole 566C is the deepest hole (136.6 m) of the four drilled at this site and contains the oldest marine sediments on serpentinite basement. Sample 566C-H1,CC, a wash core recovered from a depth of approximately 50 m, contains a mixed Pliocene–Pleistocene assemblage, which is composed of small *Gephyrocapsa* spp., *Heliosphaera kamptneri*, and very rare *Discoaster pentaradiatus*.

Samples 566C-1,CC through 566C-3,CC contain *Discoaster berggreni*, *Discoaster quinqueramus*, and *Sphenolithus neoabies* and are assigned to the late Miocene *Discoaster quinqueramus* Zone. Very rare reworked Cretaceous species are present in 566C-2,CC whereas 566C-3,CC contains very rare reworked *Micula mura*, a species restricted to the late Maestrichtian.

No sediment was recovered from Core 566C-4, and a wash core (566C-H2) taken at approximately 109 m contains the same late Miocene nannnofossils as previously

encountered uphole. Cores 5 through 7 once again contain serpentinite.

Diatoms

Biostratigraphically useful species present in cores from Holes 566, 566A, and 566C, are *Actinocyclus ellipticus*, *Rossiella tatsunokuchiensis*, *Nitzschia reinholdii*, *Pseudoeunotia doliolus*, *Roperia tesselata*, and *Rhizosolenia praebergonii*. *P. doliolus* appears at the beginning of the Olduvai Event of the lowermost Pleistocene (Burckle, 1977a) and is a reliable Pleistocene zonal marker. The first five cores from Hole 566 contain abundant well preserved *P. doliolus*.

Hole 566

The diatom *Rhizosolenia praebergonii* became abundant just before the Olduvai and became extinct just after the Olduvai. It is considered a good marker for equatorial regions for the Olduvai Event, at the Pliocene/Pleistocene boundary (Burckle, 1977a). Concurrent occurrences of *Pseudoeunotia doliolus* and *R. praebergonii* in Cores 3 through 5 define a lowermost Pleistocene Sub-
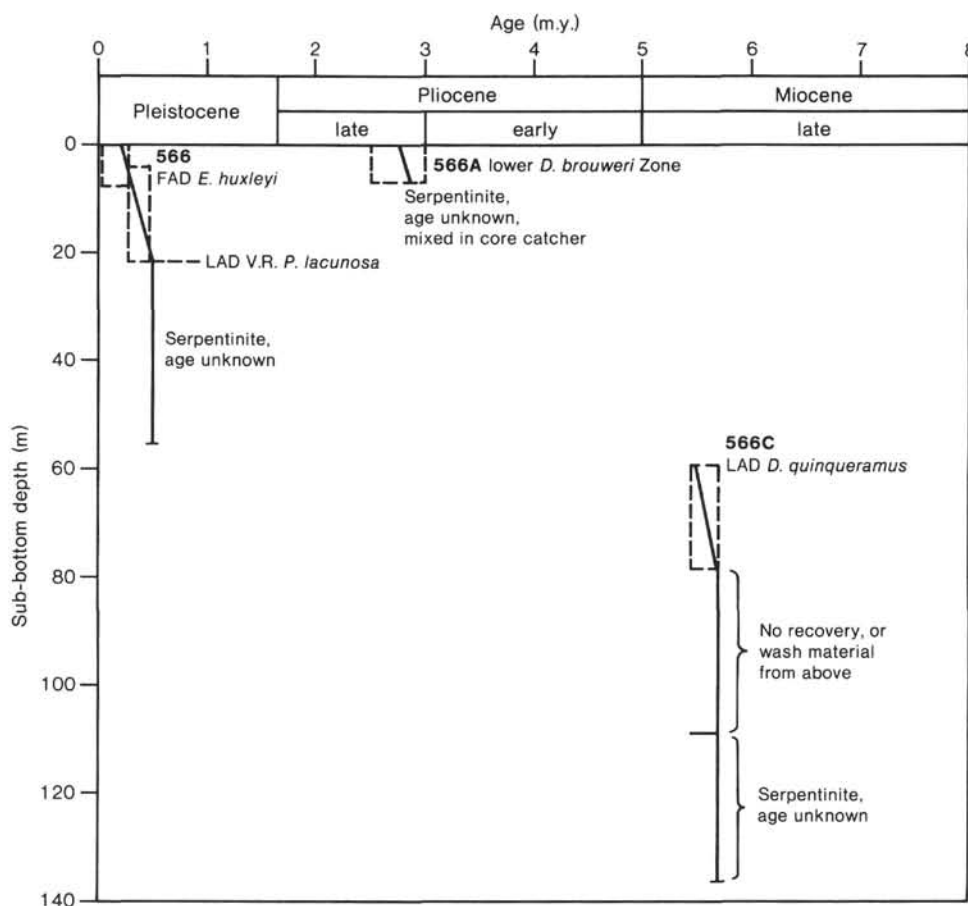
Figure 6. General sediment accumulation rates uncorrected for compaction for Holes 566, 566A, and 566C. For all three holes, sediment accumulation rates are ≈ 75 m/m.y. V.R. = very rare.

zone. The last occurrence of *Nitzschia reinholdii*, which took place in the early Brunhes (Burckle, 1977a), allows it to be used as a lower Pleistocene zonal marker also. It was observed in Cores 2 through 5.

Bukry and Foster (1973) defined a *Roperia tesselata* Zone for the upper Pleistocene in the Panama Basin. Burckle (1977a) places this zone, corresponding to the lower Brunhes, above the last occurrence of *Nitzschia reinholdii*, which is Section 566-2-4 at this site. *Roperia tesselata* was recorded from Section 566-2-3.

Hole 566A

The single core-catcher sample from Hole 566A contained the marker fossils *Nitzschia jouseae* and *Thalassiosira convexa*. *Nitzschia jouseae* has been established as a reliable indicator of the middle and late early Pliocene (Burckle, 1972). It occurs in good condition in the core-catcher sample of 566A. *Thalassiosira convexa*, a late Pliocene species, describes the *Nitzschia jouseae* Zone attributed to the middle and late early Pliocene (Burckle, 1977b). This diatom was observed in Hole 566A, but no estimation of abundance could be made because of the general paucity of diatoms in the sample.

Hole 566C

The first four core-catcher samples recovered from this hole (H1, 1, 2, 3) are diatomaceous. A total of twelve

species was observed. Biostratigraphically significant taxa are *Rossiella tatsunokuchiensis* (present in H1 and 1,CC) and *Hemidiscus ovalis* (present in 1,CC), both of which became extinct in the late Miocene. *Annellus californicus*, a species common in 566C-3,CC, is a robust cosmopolitan form reportedly useful in pan-Pacific correlations of early middle Miocene sediments because of its short range (Burckle, 1977b). Its occurrence in this interval implies reworking from older strata.

Benthic Foraminifers

Hole 566

Only late Pleistocene faunas were encountered in Hole 566. The Pleistocene interpretation is based on the absence of older extinct species and the similarity of the faunas to the Holocene assemblages of Smith (1964). The fossil assemblages suggest that deposition occurred at lower bathyal depths (2000–4000 m). Various lower bathyal forms such as *Gyroidina soldanii*, *Melonis pompilioides*, *Pullenia bulloides*, and *Uvigerina hispida* are present. The bulk of the assemblages in the fossiliferous portion of this site is composed of upper bathyal and upper middle bathyal species, particularly those species adapted to low oxygen conditions (*Bolivina seminuda*, *B. beyrichi*, and *Buliminella subfusiformis*). Transported

specimens from the outer shelf and lower slope are also present, as are very rare abyssal forms.

Hole 566A

Recovery from this hole was extremely poor. The single specimen of *Cibicides fletcheri*, a pyritized *Globobulimina pacifica*, and a *Bulimina* fragment indicate only a late Tertiary age. The depth of deposition was probably greater than 1200 m given the preferred habitat of *G. pacifica* and the pyritized nature of the test.

Hole 566C

Benthic foraminiferal assemblages in Wash Cores H1 and H2, and Cores 1 through 3 suggest an age of early Pliocene to late Miocene for the fossiliferous portion of this hole. Benthic foraminifers favor the early Pliocene interpretation because of the continued abundance of *Bolivina pseudospissa*, which is usually absent in the late Miocene assemblages, and because the first downhole appearance of *Bulimina uvigerinaformis* in 566C-2,CC indicates the late Miocene. This age is further corroborated by the nannofossils and the appearance of *Sphaeroidina bulloides*, *Pleurostomella alternans*, and other Miocene species in 566C-2,CC and subsequent cores.

Benthic foraminifers throughout the fossiliferous interval indicate deposition occurred in the abyssal biofacies (4000 m). Faunas in Wash Core 566C-H2 and 566C-2,CC and 566C-3,CC are poorly preserved, rare, and associated with a fine sand. These assemblages are composed primarily of transported outer shelf and upper slope specimens, which are approximately the same size as the sand grains. Wash Core 566C-H1 has a similar abyssal fauna and transported upper slope fauna. This assemblage, however, is associated with the mud and not

size sorted, as are the older assemblages. Abyssal benthic foraminifers in Core 566C-1 are rare, and poorly preserved. These specimens are associated with rusty colored grains and together suggest a slower sedimentation rate and considerable weathering and/or reworking of the sediment.

PHYSICAL PROPERTIES

Methods

Physical properties measurements were performed similarly to those at Site 565. Gravimetric determinations of bulk density and porosity, however, were obtained utilizing the rock-chunk technique, weighing the sample in air and submersed in water. In addition, unconfined compression tests were done using a hand-held Soil Test penetrometer. These two tests were performed parallel to the bedding plane in split cores. Thermal conductivity measurements were also done following the standard shipboard technique (Hyndman et al., 1974).

Results

Bulk density, wet-water content, and void ratio (porosity) values are presented in Figure 7. The bulk density increases slightly from 1.43 Mg/m^3 near surface to 1.66 mg^3 at 24.3 m, with corresponding slight decreases in water content and porosity. Two-minute GRAPE densities are consistently lower than those determined gravimetrically, which may result from using an improper grain density in the computation.

Shear strength and penetrometer test results are shown in Figure 8; shear strengths vary between 47 kPa to 83 kPa in the upper 15 m. The values for these parameters parallel one another nicely except for the sample recorded
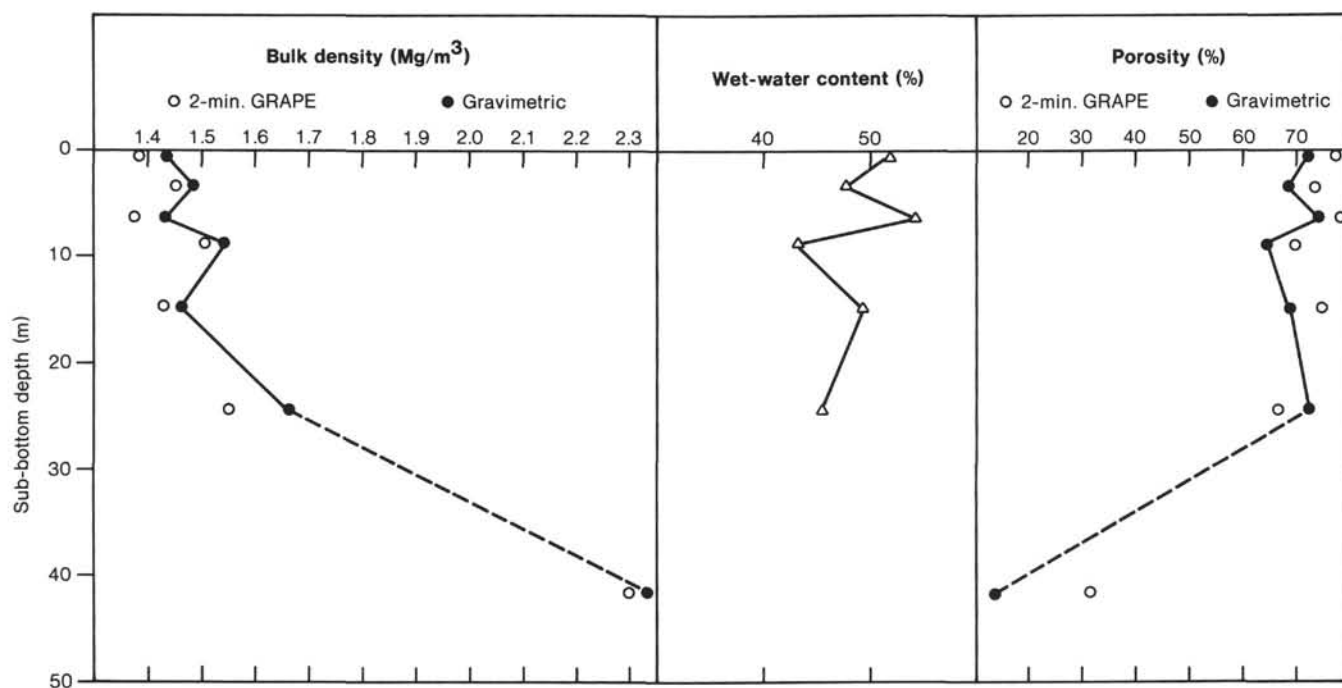

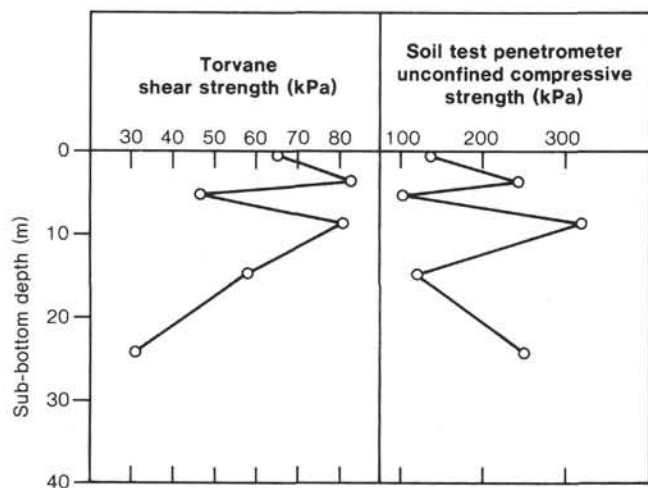Figure 7. Index properties of cored material at Site 566.

Figure 8. Variation of strength measurements for sediments from Site 566.

at 24.3 m. The values obtained show extraordinarily high strengths for such shallow sediments, suggesting over-consolidation.

Sonic velocities and acoustic impedance values for the sediment cover at Site 566 show very little variation (Fig. 9). There is an overall increase in sonic velocity from 1.531 km/s at the surface to 1.589 km/s at 24.3 m. These values approach those measured by downhole logging of Hole 566C, which ranged between 1.6 and 1.7 km/s overall.

Results of bulk densities, sonic velocities, and acoustic impedance for the serpentinized peridotites are shown in Table 2. The maximum velocity obtained for the serpentinized samples is 5.268 km/s and corresponds to the least fractured or altered material sampled. These velocities match well with those obtained previously from

refraction work for basement material along this part of the Trench (Ambos et al., 1981; Ibrahim et al., 1979).

Thermal conductivity measurements (Table 3) show an average of 1.76 mcal/cm°C · s for the sediment cover. The values shown are not corrected to *in situ* conditions. Poor contact between the probe and the serpentinite sample cast a question on this measurement of conductivity.

Discussion

The thin sediment cover at Site 566 is characterized principally by the high shear and compressive strengths found as well as the low void ratios, which suggests an overconsolidated state. This state may have resulted from removal of overburden and/or fabric rearrangement produced by slumping or mass movement. This latter mechanism is revealed biostratigraphically as displaced foraminiferal assemblages. Lithostratigraphic findings suggest slump movement occurred as a unit because internal stratification is not disrupted in the upper unit and erosional processes are dominant in formation of sedimentary structures. The likely explanation of observations at this site is that there was a succession of slump block units with different degrees of removed overburden resulting from current or downslope transport sweeping mechanisms, thus revealing the trends suggested by physical properties and lithostratigraphic and biostratigraphic studies.

Downhole Logging

Three log passes were performed in Hole 566C although blockage within the hole unfortunately limited these logs to the interval between 17.5 and 66.0 m sub-bottom. Sonic velocity and natural gamma-ray measurements were collected.

The natural gamma-ray records seem to reflect two lithologies at this site that may be mudstone and sand-
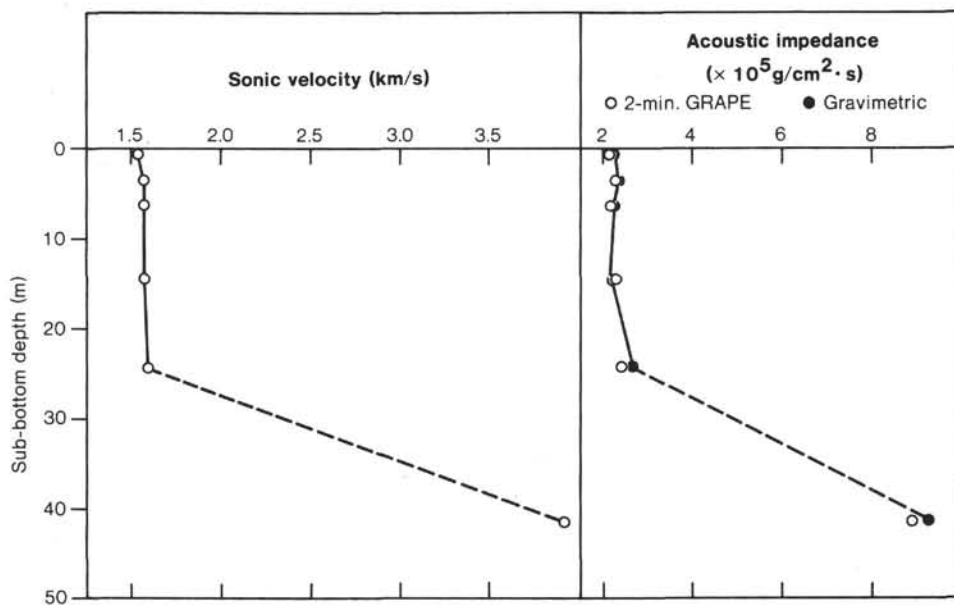

Figure 9. Acoustic characteristics of recovered sediments and rock at Site 566.

Table 2. Physical properties of serpentinized peridotites at Site 566.

Section (hole-core-section)	Sub-bottom depth (m)	Bulk density[a] (Mg/m³)	Sonic velocity[b] (km/s)	Acoustic impedance[a] (x 10⁵ g/cm² · s)
566-7-1	41.5	2.366 (2.303)	3.091	9.230 (8.984)[a]
566A-1-1	7.0	2.493	4.485	11.181
566C-5-1	109.1	2.515 (2.361)	3.990	10.035 (9.420)
566C-6-1	117.7	2.624 (2.497)	5.268 [5.099]	23.823 (13.154)
566C-7-1	127.7	2.520 (2.476)	4.184	10.544 (10.360)

[a] 2-minute GRAPE data are in parentheses; other data are gravimetric.
[b] Measured perpendicular to bedding; brackets indicate measured parallel to bedding.

Table 3. Thermal conductivity of sediments from Site 566.

Section (hole-core-section)	Thermal conductivity (mcal/cm°C · s)
566-2,CC	1.76
566-4,CC	1.84
566-5-2	1.67
566-8-1	6.567

stone. Two possible sandstone units are reflected in these records between 44.0 and 46.5 m and 51.0 and 53.5 m sub-bottom. The data between 32.0 and 42.0 m may be indicative of interbedded sands and mudstones, possibly grading upward from more sand layers to predominately mud at the top of the section.

The sonic velocity logs are somewhat erratic in places, a probable result of attenuated signals, as may be appreciated in the waveform records. Nevertheless, the logged section shows velocities varying around 1.7 km/s for the first pass and 1.6 km/s during the second pass, which is close to those velocities measured for slope mudstone in the laboratory at Site 566. Velocities computed during the first run for the bottom of the section were obtained while the tool was stationary and are on the order of 1.83 km/s. This velocity and the nature of the gamma-ray log suggest highly consolidated mudstone, which is the major lithologic constituent drilled at Holes 566, 566A, and 566C.

GEOPHYSICS

The geophysical information from Site 566 consists of a regional and local bathymetry, total field magnetic data, orthogonal lines of multichannel seismic reflection data that intersect at the site, and regional seismic refraction measurements. These data are presented here as they pertain to the site and have also been discussed in other papers (Ibrahim et al., 1979; Ladd et al., 1982; von Huene et al., 1982).

Bathymetry

The map of regional bathymetry made by McMillan et al. (1981) from the University of Texas site survey data shows Site 566 in the lower reaches of San José Canyon where the Canyon becomes relatively shallow and has a poorly defined course (Fig. 1). The *Glomar Challenger* ran lines spaced 3 to 3.5 km paralleling the slope while the ship was standing by waiting for permission to drill off Guatemala. The *Challenger* survey and lines made

while coming on site were navigated more precisely and are more closely spaced than the University of Texas data (Fig. 10). The local map shows a simple wide canyon, and seismic record GUA-2 runs along the eastern bank. The canyon bottom is marked by a complex rough topography near the site, suggesting erosion of hard rock or nondeposition. This is consistent with the hard rock recovered by conventional sampling of gravels containing chert, basalt, and serpentine (McMillen et al., 1981).

Total Field Magnetic Anomalies

The map of magnetic anomalies (Fig. 11) shows the relatively smooth Earth's total magnetic field around Site 566. This smooth magnetic field is in contrast to the linear anomalies over ocean crust on the seaward side, and the sharply varying anomalies of high intensity over the edge of the shelf and the upper slope on the landward
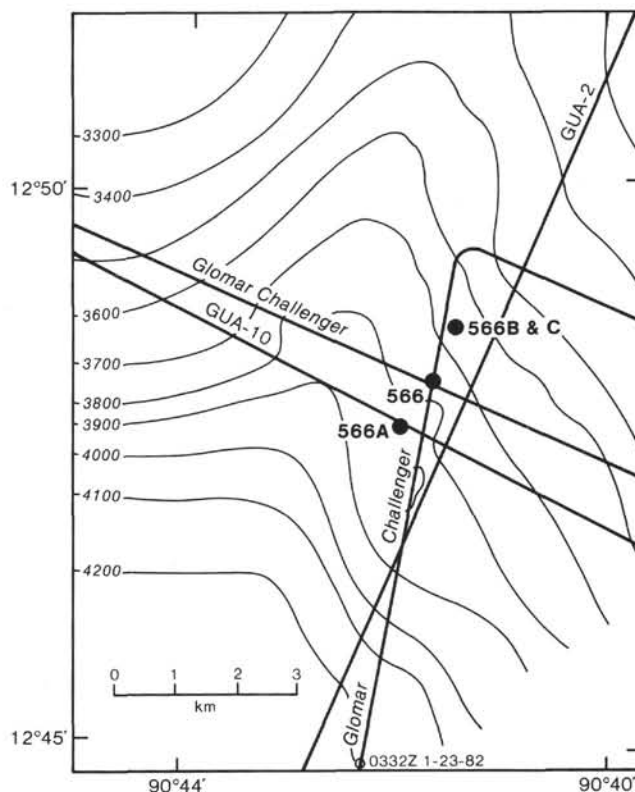

Figure 10. Local bathymetry around Site 566 from records made by the *Glomar Challenger* and by the University of Texas (GUA-2 and -10).
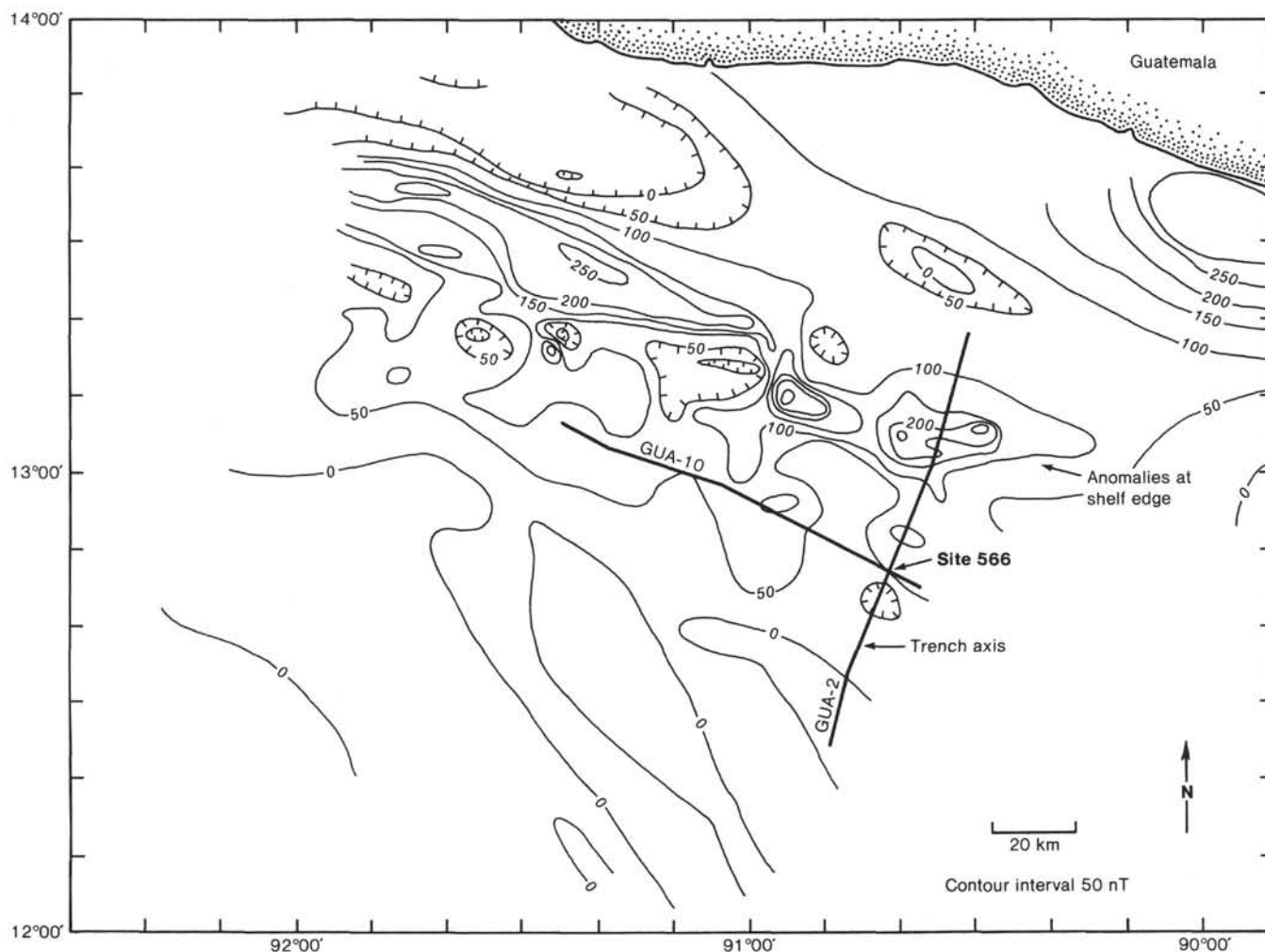
Figure 11. Regional map of magnetic anomalies showing location of Site 566 and University of Texas seismic lines.

side. The uncorrected magnetic anomalies measured by *Glomar Challenger* when coming on site increase 140 gamma from the Trench to the site, and over this 22 km they deviate from linearity no more than 10 gamma. There is no indication of the shallow depression near Site 566 shown on the regional map (Fig. 11).

Seismic Records

Site 566 was positioned close to the intersection of University of Texas seismic lines GUA-2, which runs down the slope, and GUA-10, which runs across it (Figs. 10 and 11). GUA-2 has been used to show continuation of ocean crust 30 km landward from the Trench (Ladd et al., 1978; 1982). Ladd et al. (1978; 1982) argue that the recording of this reflection indicates deep penetration of seismic energy (Fig. 12). The general lack of reflections between the ocean floor and the base of the upper plate therefore suggest lack of coherent reflectors or a velocity contrast.

GUA-2 has been redisplayed and was also migrated to better define the thickness of slope deposits. The base of slope deposits has been highlighted in Figure 12 (a nonmigrated version), as has the top of the ocean crust. Much of the intervening part of the record is masked by

diffractions and reverberations, but faint reflections were recognized (Fig. 12). Some are reflections, some diffractions, and they are not sufficient to resolve a good structural interpretation . Both landward- and seaward-dipping structure is allowable, depending on the case preferred from other data. Although the slope deposits do level some of the underlying irregularities, the base of slope deposits is a surprisingly regular surface; the development of such a surface by a deep marine process is indeed puzzling.

GUA-10 trending parallel to the slope profiles San José Canyon. The axial portion is without much sediment; the banks are slope deposits with reflections of low amplitude that are not clearly seen through the diffractions that mask them. Thus there is little structural information to determine whether the banks are erosional or constructional, however, the rather uniform thickness of the slope deposits and lack of levees suggests predominance of erosion. The generally irregular stratification of the slope deposits is consistent with the evidence of abundant mass movement in core from this environment.

Below the base of the slope deposits only reflections from the top of the oceanic crust can be identified (be-
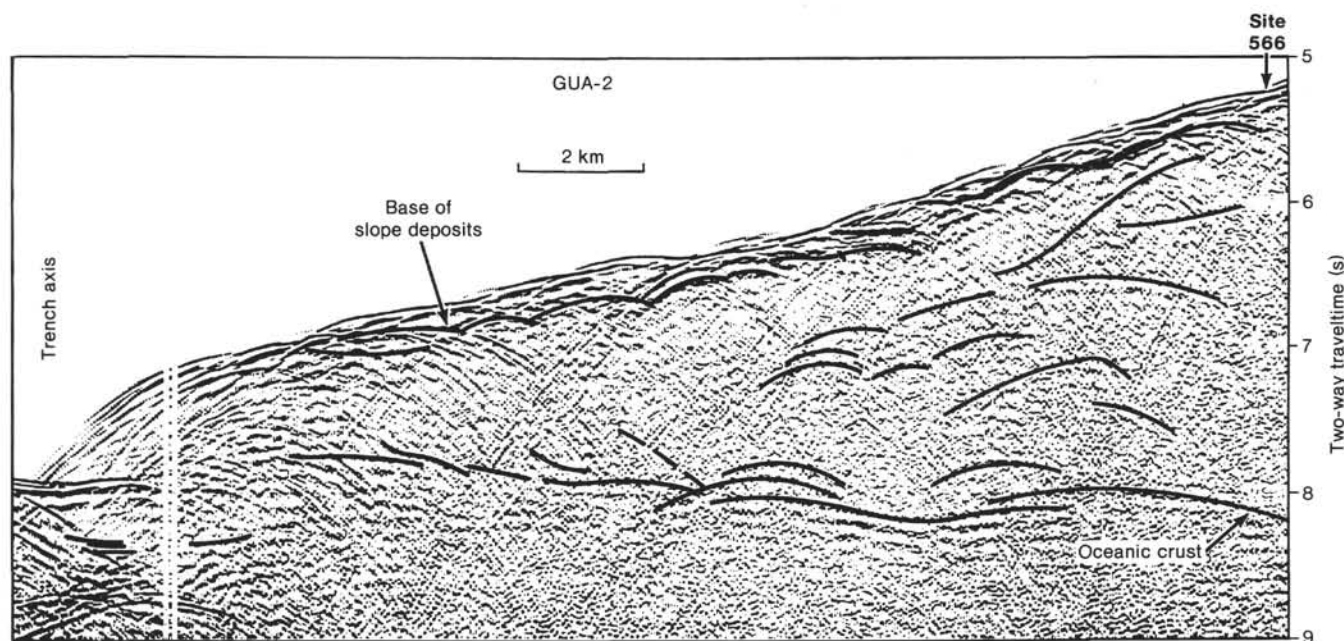
Figure 12. Seismic record GUA-2, showing interpretation with emphasized reflections.

low base of record in Fig. 12). None of the faint reflections can be recognized as geologic structure with even modest confidence. It should be noted, however, that the processing of seismic data in GUA-10 was not as good as that in GUA-2, and perhaps this factor accounts for the lesser information content in GUA-10.

Seismic Refraction

Two refraction experiments off Guatemala show the general velocity structure of the slope near Site 566. Ibrahim et al. (1979) report an OBS (ocean-bottom seismometer) station to the northwest of Site 566 where the shots were made along a line paralleling the slope. At the base of the slope deposits, a compressional velocity of 3.0 km/s is followed by a 4.7-km/s velocity at the top of the oceanic crust, 6.2 km below the seafloor. Another OBS refraction experiment by the Hawaii Institute of Geophysics was reported by Ambos (1981). Refraction measurements were made shooting perpendicular to the slope and receiving on an array of instruments centered about Site 494. At the equivalent position of Site 566, the velocity structure consists of a gradational increase from 3.0 km/s near the surface to 4.8 km/s at the base, which is also 6.2 km below the seafloor. The two experiments agree almost perfectly in this part of the crust. Within the igneous ocean crust, however, the Texas data show a velocity of 6.8 km/s and the Hawaii data indicate a 5.3-km/s velocity increasing gradually downward. This discrepancy may show the heterogeneity of the lower crust or a difference in the data and their analysis.

Conclusions

The position of Site 566 in San José Canyon allowed recovery of lithologies below the slope deposits without extensive drilling. The recovery of serpentinite was surprising and could not have been anticipated from the geophysics alone. First, the refraction velocities 3.0–4.8 km/s are less than the reported measurements of velocities of serpentinite ranging between 4.7 and 6.4 km/s. This difference suggests that although some less weathered pieces of peridotite were recovered, the bulk of this unit is probably highly serpentinized. Second, the lack of magnetic anomalies above rock with seismic velocities greater than 2 km/s is more typical of a consolidated sediment. The possibility that the body drilled at Site 566 is only local is counter to the recovery of serpentinite at three other DSDP sites on the slope, the recovery of serpentinite in two conventional cores nearby, and perhaps to the absence of a change in the velocity structure along two orthogonal refraction lines.

The lack of seismic reflections in the full 6 km of upper plate below the site is consistent with the recovery of serpentinite. The structure in serpentinite sequences is generally irregular; and at the scale of 50 m or more, which is the limit of resolution of the seismic instrument system used, strong reflections would not be expected. However, some of the faint reflections in GUA-2 suggest a structural geometry subparallel to the ocean floor or the top of the oceanic crust.

PALEOMAGNETISM

Oriented 7-cm^3 samples were taken at an average stratigraphic interval of 50 cm throughout all suitable undisturbed sections of sedimentary cores. Also, two 2.5-cm-diameter oriented cores were taken from two of the cores that penetrated basement rock in Hole 566C. The results of alternating field (AF) demagnetization experiments on selected samples are shown in Figure 13. The sedimentary samples are reasonably stable, although the inclinations of the first two samples from Core 1 both
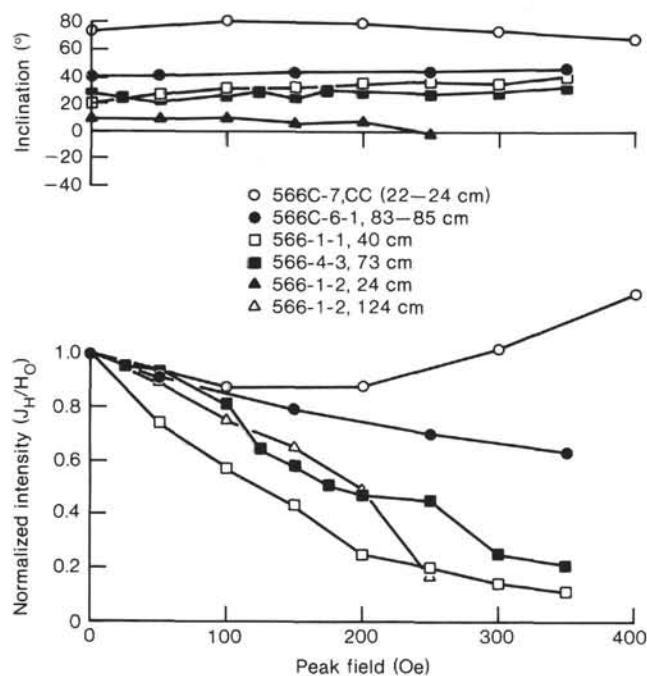
Figure 13. Results of AF demagnetization on selected samples from Holes 566 and 566C.

Figure 14. Results of thermal demagnetization on the two serpentinite samples.

show a slight rotation away from the direction of the present field, which has an inclination of 40° at this site. The first serpentinite sample (566C-6-1, 83–85 cm)[3] is very stable to AF demagnetization up to peak fields of 350 Oe. At fields greater than this, the intensity increases rapidly, due to acquisition of an anhysteretic remanent magnetization (ARM), which may be caused by lack of symmetry in the demagnetizer waveform. The inclination remains stable up to fields of 350 Oe. It is very close to the inclination of that of the present field at this site (40°). However, this inclination is calculated relative to a plane at right angles to the core. Because the core it was taken from was inclined at 10.5° to vertical, the inclination relative to the true horizontal could be between 30° and 50°.

The second serpentinite sample, 566C-7,CC (22–24 cm), has an NRM inclination that is close to vertical (75°). Changes in direction are fairly small up to fields of 300 Oe, but the increases in intensity at fields greater than this indicate acquisition of an ARM in this sample at even lower peak fields than for the first sample.

Results of thermal demagnetization experiments on the two serpentinite samples are presented in Figure 14. The directions of magnetization are very stable in both samples up to temperatures of 450°C. At temperatures greater than this, the intensities drop rapidly, indicating a Curie point of between 550 and 600°C for Sample 566C-6-1, 83–85 cm close to that of magnetite (565°C). The anomalous increase in intensity of Sample 566C-7,CC (22–24 cm) at 450°C and its relatively high intensi-

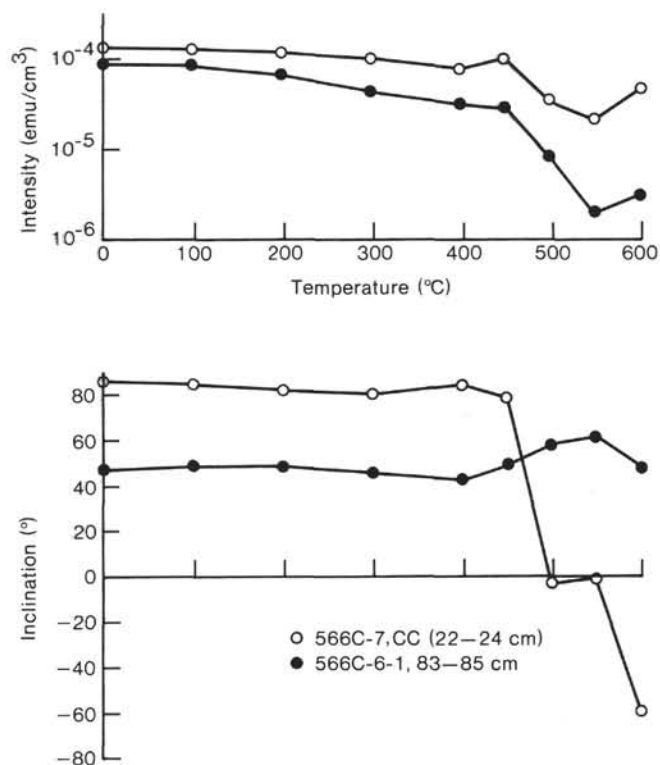ty at 500 and 550°C may be caused by acquisition of a TRM (thermal remanent magnetization) in the small residual field in the cooling chamber of the furnace (< 10 gamma). The results at 600°C clearly indicate acquisition of similar TRMs by both samples. It was found that rather large fields (> 1000 gamma) exist in this chamber. They are produced by the heating coils in the unit. Results of susceptibility measurements on the two samples and resulting Königsberger ratios—Q_n—are shown in the table below. The Königsberger ratio is the ratio of natural remanent magnetization to magnetic susceptibility times the present geomagnetic field intensity (about 0.4 Oe). The relatively low values of both NRM (natural remanent magnetization) and Q_n are consistent with the lack of magnetic anomalies observed in the vicinity of Site 566.

Sample (interval in cm)	NRM ($\times 10^{-4}$ emu/cm³)	Susceptibility ($\times 10^{-4}$ cm·g·s)	Q_n
566C-6-1, 83–85 cm	1.4	4.5	0.78
566C-7,CC (22–24 cm)	5.0	19	0.66

Results of NRM measurements on the sedimentry sequence overlying the serpentinites are plotted in Figure 15. The results indicate normal polarities down to the base of Core 5 where there is a possible reversal. The offsets in the declinations are artificial, as absolute azimuthal orientation data were only available for Core 2.

[3] The first serpentinite sample, 566C-6-1, 83–85 cm, was recovered from a brecciated core; its position in the total core length may have been anywhere from 0.5 to 8 m from the top of the core.
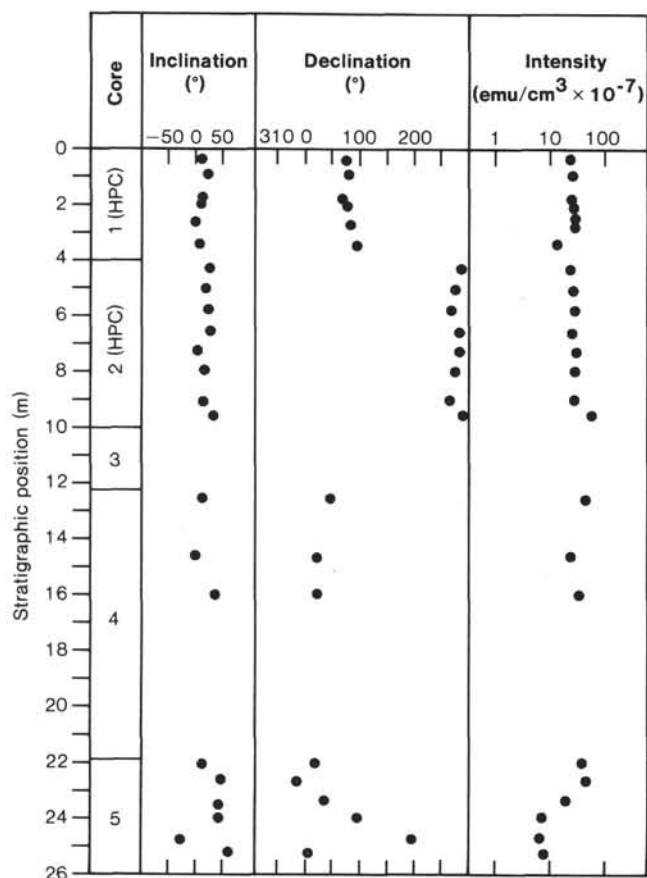
Figure 15. Stratigraphic plot of NRM data for Hole 566.

The consistency in the data for the two HPC cores is impressive, although the variations in inclination indicate that caution must be used in interpreting magnetic polarities from inclination data alone at low latitudes.

GEOCHEMISTRY

Hole 566

Drilling at the first hole at Site 566 on the lower slope of the landward wall of the Middle America Trench off Guatemala immediately encountered stiff mud followed by serpentinite. No gas samples were obtained through the core liner; samples of mud were recovered between 3.0 and 15.3 m for headspace gas analyses (Kvenvolden and McDonald, this volume). Chemistry of the interstitial water from three samples is shown in Table 4.

Hole 566C

Gas was first observed within the core liner of Core 6. Rubble associated with fractured serpentinite degassed vigorously. No discrete gas pockets were present, and the gas had free communication with the ends of the core liner. A sample of the gas was taken through a puncture in the core liner with a standard vacutainer at the point of most obvious gas release (sub-bottom depth 118.4 m). The resulting sample (Table 5) was composed of 49% C_1, a rather large value considering the ample opportunity for air contamination through the ends of the core liner. More surprising, however, were the high concentrations of C_2, C_3, and i-C_4, with much lower but still significant concentrations of higher molecular weight hydrocarbon gases (Table 5). Core 7 showed no obvious degassing, and any gas could easily have escaped through the ends of the core liner. Nevertheless, a sample of gas was taken through the core liner with a vacutainer at 127.8 m sub-bottom depth, and the results are similar to those obtained for Core 6 (Table 5).

The relative concentrations of all gases are very high, especially for samples taken at shallow sub-bottom depths of less than 130 m. The gases probably were not generated in place, but rather may have been derived from thermal decomposition of organic matter and migrated from sediments that are or have been more deeply buried. The migrating gases collected within the fractures of the serpentinite.

SUMMARY AND CONCLUSIONS

Summary of Drilling

Site 566 is 22 km upslope from the axis of the Middle America Trench and about 2300 m above it. The site was positioned to sample the acoustic basement at the top of the lower slope of the Trench. The lower slope is charac-

Table 4. Chemistry of interstitial water, Hole 566.

Core-section	Sub-bottom depth (m)	pH	Alkalinity (meq/l)	Salinity (‰)	Calcium (mmoles/l)	Magnesium (mmoles/l)	Chlorinity (‰)
1-2	3.0	7.73	4.59	33.2	11.5	47.3	19.14
2-3	8.5	7.59	9.81	32.0	16.0	47.5	18.97
4-2	15.3	7.65	11.64	32.9	11.2	47.6	18.97

Table 5. Distribution of hydrocarbon gases, Hole 566C.

Core-section	Sub-bottom depth (m)	C_1 (%)	C_2 (ppm)	C_3 (ppm)	i-C_4 (ppm)	n-C_4 (ppm)	neo-C_5 (ppm)	i-C_5 (ppm)	n-C_5 (ppm)
6-1	118.4	49	1200	560	540	29	2.4	5.3	3.9
7-1	127.8	45	2800	1400	1500	110	7.9	36.0	4.3

terized by a smooth seafloor of uniform dip that has only locally been modified by a sequence of steps or by the subduction of ridges on the incoming ocean floor, which have disturbed the topography of the Trench–slope juncture. The smooth seafloor reflects an underlying smooth acoustic basement surface upon which a 200- to 400-m thick blanket of slope sediment has been deposited. To reduce the possibility of drilling a slope deposit sequence containing gas hydrate, the site was positioned in San José Canyon where seismic reflection records show thin sediment. Three holes (566B had no recovery and is not considered here), aligned along the eastern side of the Canyon axis and spaced 1 km apart, were drilled to test the lateral variability of the basement over a 2-km distance across the strike of the slope (Fig. 16).

In the original IPOD program, a Seabeam site survey of San José Canyon was planned prior to drilling on Leg 84, but in the Planning Committee reorganization of Pacific drilling in the 1981–1983 program, the Guatemalan drilling was advanced one year; the Seabeam survey could not be similarly advanced and so was completed afterward. While waiting for permission to drill, the *Challenger* was used to make a bathymetric survey around the site. The *Challenger* survey allowed corrected positioning of the site in sediment sufficient for spudding but not thick enough for gas hydrate.

Poor core recovery (2–38%), interval coring, and the inability to log more than 48 m of Hole 566C preclude definition of a comprehensive slope-deposit lithostratigraphy; however, the recovery of ultramafic basement fulfilled the primary objective at this site. The ultramafic rock was originally mainly harzburgite and lherzolite, as shown by structure and mineralogy. The upper surface is now a highly altered serpentinite, with carbonate filling the microfractures. The weathered serpentinite grades downward to serpentinite and then serpentinite with about 20% original minerals. Secondary minerals indicate low-temperature alteration (probably below 300°C); the sheared and foliated nature of the rock indicates stress, probably during the alteration. The low-temperature alteration may be an explanation for the low magnetic susceptibility measured on samples of serpentinite.

The slope and canyon deposits consist of massive mudstone, pebbly mudstone, laminated muds, and graded sandstone. Deposition involved both current activity and mass movement of sediment derived from sources upslope. Reworked benthic foraminifers, from environments about 1500 to 2500 m deep, are numerous, and
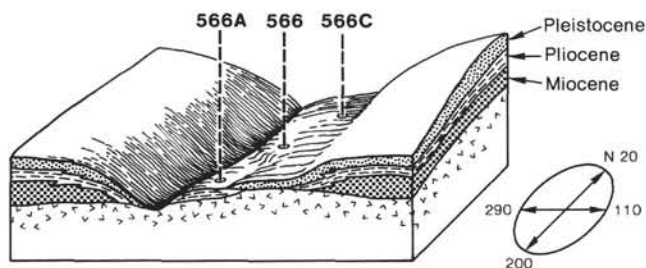
some Miocene intervals have reworked Cretaceous nannofossils. Sandstone composition, rich in arc-derived components, suggests that San José Canyon has been a transport path from the shelf to the Trench since at least the late Miocene. The sediment appears overconsolidated, possibly caused by erosion of an overlying section. This idea is consistent with early signs of fracturing.

The biostratigraphy demonstrates that slope deposits of different ages cover basement in the Canyon. At Hole 566 the oldest cover is Pleistocene; at 566A, Pliocene; and at 566C, late Miocene. Basement probably crops out in the canyon. The different-aged cover also reflects active erosion and deposition in San José Canyon.

The amount of gas in the sediment was small and insufficient for the development of gas hydrate. However, an unexpected occurrence of gas was noticed in the serpentinite of Hole 566C. It consisted of 45% methane, 2800 ppm ethane, 1400 ppm propane, 1500 ppm isobutane, 110 ppm *n*-butane, 40 ppm isopentane, and 4 ppm *n*-pentane.

Conclusions

The recovery of ultramafic rock at Site 566 was unanticipated on the basis of the geophysical data, because the refraction velocities are lower than laboratory values for serpentinite and the magnetic anomaly field is featureless. A serpentinite body is not inconsistent, however, with the geophysical data; what was not anticipated is the apparent altered state of this serpentinite in a deep submarine environment, and the absence of magnetic mineralization because of the low-temperature alteration. The possibility that the body of ultramafics is only a local one is inconsistent with the following: (1) the 2-km minimum extent at the site shown by the drill holes, (2) the prior recovery of serpentinite 20 km away by the *Ida Green* (Ladd et al., 1978) and its recovery at four other Leg 84 sites, and (3) the apparent absence of any change in velocity structure along two orthogonal nearby refraction lines. The featureless magnetic anomaly field and consistent lack of reflections in the seismic data allow the inference that much of the lower slope is composed of serpentinite.

The position of Site 566 in San José Canyon where slope sediment has been eroded precluded recovery of the oldest slope deposits on the serpentinite. Therefore, the late Miocene slope sediment at Hole 566C probably reflects only the last erosional episode there.

To find an ultramafic body from the mantle at the front of a convergent margin is puzzling. The sequence of tectonic events needed to explain such a location is likely to involve much more than just simple subduction or obduction. From regional geology, it seems likely that the Site 566 ultramafic is an extension of the crustal complex that underlies much of Central America south of the Polochic–Motagua fault zones.

Figure 16. Three dimensional block diagram of San José Canyon and Holes 566, 566A, and 566C.
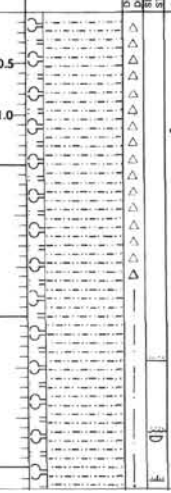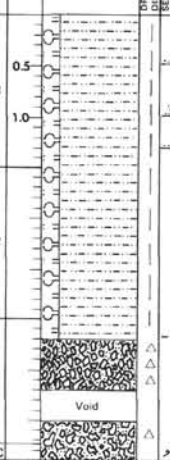
REFERENCES

Ambos, E. L., Hussong, D. M., and Carter, J. A., 1981. Seismic refraction results from the lower slope of the Middle America Trench offshore Guatemala. (Abstract) *Trans. Am. Geophys. Union*, pp. 1042.
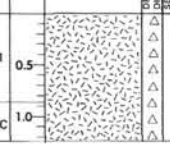
Bukry, D., and Foster, J. H., 1973. Silicoflagellate and diatom stratigraphy, Leg 16, Deep Sea Drilling Project. *In* van Andel, Tj. H., Heath, G. R., et al., *Init. Repts. DSDP*, 16: Washington (U.S. Govt. Printing Office), 815–871.

Burckle, L., 1972. Late Cenozoic planktonic diatom zones from the eastern equatorial Pacific. *First Symposium on Recent and Fossile Marine Diatoms*, Nova Hedwigia, 39.

————, 1977a. Pliocene and Pleistocene diatom datum levels from the equatorial Pacific. *Quat. Res.*, 7:330–340.

————, 1977b. Early Miocene to Pliocene diatom levels for the equatorial Pacific. Proceedings of the Second Working Group Meeting, biostratigraphic datum-planes of the Pacific Neogene. IGCP Project 144. *Republic of Indonesia, Ministry of Mines and Energy, Spec. Publ. No. 1*, pp. 25–44.

Haq, B. U., Worsley, T. R., et al., 1980. Late Miocene marine carbon-isotope shift and synchroneity of some phytoplanktonic biostratigraphic events. *Geology*, 8:427–431.

Hyndman, R. D., Erickson, A. J., and Von Herzen, R. P., 1974. Geothermal measurements on DSDP Leg 26. *In* Davies, T. A., Luyendyk, B. P., et al., *Init. Repts. DSDP*, 26: Washington (U.S. Govt. Printing Office), 451–464.

Ibrahim, A. K., Latham, G. V., and Ladd, J. W., 1979. Seismic refraction and reflection measurements of the Middle America Trench offshore Guatemala. *J. Geophys. Res.*, 84:5643–5649.

Ladd, J. W., Ibrahim, A. K., McMillen, K. J., Latham, G. V., and von Huene, R. E., 1982. Interpretation of seismic reflection data of the Middle America Trench offshore Guatemala. *In* Aubouin, J., von Huene, R., et al, *Init. Repts. DSDP*, 67: Washington (U.S. Govt. Printing Office), 675–690.

Ladd, J. W., Ibrahim, A. K., McMillen, K. J., Latham, G. V., von Huene, R. E., Watkins, J. E., Moore, J. C., and Worzel, J. L., 1978. Tectonics of the Middle America Trench offshore Guatemala. *Int. Symp. of the Guatemala 4 February Earthquake and Reconstruction Process*, Guatemala City, May 1978 (Vol. 1).

McMillen, K. J., et al., 1981. *In* Leggett, J. K., (Ed.), *Trench Forearc Geology: Sedimentation and Tectonics in Modern and Ancient Active Plate Margins*. Geol. Soc. London, Spec. Publ., 10.

Saito, T., Burckle, L. H., and Hays, J. D., 1975. Late Miocene to Pleistocene biostratigraphy of equatorial Pacific sediments. *Lamont-Doherty Geological Observatory Contribution No. 2223*, pp. 226–244.

Schrader, H. -J., 1972. Stratigraphic distribution of marine *Denticula* species in Neogene North Pacific sediments. In *Second Symposium on Recent and Fossil Marine Diatoms, London*, Sept. 1972.

Smith, P. B., 1964. Ecology of benthonic species. *U.S. Geol. Surv. Prof. Pap. 429-B*.

von Huene, R., Ladd, J., and Norton, I., 1982. Geophysical observations of slope deposits, Middle America Trench off Guatemala. *In* Aubouin, J., von Huene, R., et al., *Init. Repts. DSDP*, 67: Washington (U.S. Govt. Printing Office), 707–718.

SITE 566   HOLE   CORE 1   CORED INTERVAL   0.0–4.0 m sub-bottom

TIME – ROCK UNIT	BIOSTRATIGRAPHIC ZONE	FOSSIL CHARACTER					SECTION	METERS	GRAPHIC LITHOLOGY	DRILLING DISTURBANCE	SEDIMENTARY STRUCTURES	SAMPLES	LITHOLOGIC DESCRIPTION
		FORAMINIFERS	NANNOFOSSILS	RADIOLARIANS	DIATOMS								

upper Pleistocene to Recent

Pseudoemiliania lacunosa–Emiliania huxleyi

Apparent dip of 20°

Mottling

Muddy sand with pyrite pebble

Erosive base to sand-parallel lamination fill the hollow

Apparent dip 22°

Mudstone pebble

Fractures beneath sand layer

Dominant lithology: 0.0–3.7 m, massive mud with some minor mottling. Color: dark olive gray (5Y 3/2). Very thin laminations present within the mud. Some bioturbation.

Minor lithology: dispersed, sandy mud. Color: dark olive gray (5Y 3/2). Graded beds up to 2 cm thick. Parallel laminated near base of bed. Often scoured base.

SMEAR SLIDE SUMMARY (%):

	1, 93	1, 98	2, 43	2, 45
	M	D	M	D
Texture:				
Sand	30	–	40	–
Silt	30	80	30	30
Clay	40	20	30	70
Composition:				
Quartz	1	–	2	1
Feldspar	2	2	5	3
Mica	–	1	–	1
Heavy minerals	5	–	1	2
Clay	40	81	55	72
Volcanic glass	2	–	–	1
Glauconite	2	–	2	1
Pyrite	3	1	10	8
Zeolite	3	–	–	–
Carbonate unspec.	10	10	20	10
Foraminifers	6	–	5	1
Calc. nannofossils	3	–	–	–
Diatoms	8	1	–	2
Radiolarians	2	Tr	–	1
Sponge spicules	2	1	–	1
Silicoflagellates	1	1	–	Tr

CARBONATE BOMB (% CaCO$_3$):
1, 92 cm = 5

SITE 566   HOLE   CORE 2   CORED INTERVAL   4.0–10.0 m sub-bottom

TIME – ROCK UNIT	BIOSTRATIGRAPHIC ZONE	FOSSIL CHARACTER					SECTION	METERS	GRAPHIC LITHOLOGY	DRILLING DISTURBANCE	SEDIMENTARY STRUCTURES	SAMPLES	LITHOLOGIC DESCRIPTION
		FORAMINIFERS	NANNOFOSSILS	RADIOLARIANS	DIATOMS								

upper Pleistocene

Pseudoemiliania lacunosa–Emiliania huxleyi

Drilling breccia

Apparent 20 dip

Fracturing of sand beds

Burrowing

Fractures

Bioturbation

Loading

Fractured sand bed with CaCO$_3$ along fracture plane

Green mottling

Sand beds (5Y 4/4)

Fractures

Convolutions

Dominant lithology: 0.0–4.7 m, siliceous mud. Color: dark olive gray (5Y 3/2). Very thin laminations and bioturbation. Tectonic fractures throughout.

Minor lithology: dispersed, muddy sand. Color: dark olive gray (5Y 3/2). Graded beds, loading. Bouma Ta and Tb.

SMEAR SLIDE SUMMARY (%):

	4, 50	4, 64
	D	D
Texture:		
Sand	15	5
Silt	15	20
Clay	80	70
Composition:		
Quartz	8	3
Mica	3	–
Clay	63	70
Volcanic glass	2	–
Glauconite	1	Tr
Pyrite	2	1
Zeolite	3	–
Carbonate unspec.	2	–
Foraminifers	–	2
Diatoms	8	10
Radiolarians	4	4
Sponge spicules	4	10
Silicoflagellates	1	–

CARBONATE BOMB (% CaCO$_3$):
1, 120 cm = 0

SITE 566 HOLE CORE 3 CORED INTERVAL 10.0–12.3 m sub-bottom

TIME – ROCK UNIT	BIOSTRATIGRAPHIC ZONE	FOSSIL CHARACTER				SECTION	METERS	GRAPHIC LITHOLOGY	DRILLING DISTURBANCE	SEDIMENTARY STRUCTURES	SAMPLES	LITHOLOGIC DESCRIPTION
		FORAMINIFERS	NANNOFOSSILS	RADIOLARIANS	DIATOMS							
upper Pleistocene	Pseudoemiliania lacunosa–Emiliania huxleyi					CC					← Small lump of mud	No recovery. Calcareous nannofossils recovered from a very small clast of mud in the Core Catcher.

SITE 566 HOLE CORE 4 CORED INTERVAL 12.3–21.9 m sub-bottom

TIME – ROCK UNIT	BIOSTRATIGRAPHIC ZONE	FOSSIL CHARACTER				SECTION	METERS	GRAPHIC LITHOLOGY	DRILLING DISTURBANCE	SEDIMENTARY STRUCTURES	SAMPLES	LITHOLOGIC DESCRIPTION
		FORAMINIFERS	NANNOFOSSILS	RADIOLARIANS	DIATOMS							
upper Pleistocene	Pseudoemiliania lacunosa–Emiliania huxleyi					1 2 3 CC	0.5 1.0					Dominant lithology: siliceous mud. Color: 5Y 3/2. Mostly structureless but some thin laminations (graded) observed. Some small dispersed sand grains. Some bioturbation.

Minor lithology: muddy sand. Color: 5Y 2/1. Mostly structureless but parallel grain alignment common. Scoured bases.

SMEAR SLIDE SUMMARY (%):
1, 117 3, 38
D M
Texture:
Sand   5   20
Silt   50 40
Clay   45 40
Composition:
Quartz   1   50
Feldspar   1   5
Mica   Tr Tr
Heavy minerals Tr –
Clay   80 35
Volcanic glass 1   1
Palagonite 1   –
Glauconite 1   2
Pyrite   2   5
Zeolite   –   1
Carbonate unspec. 2 –
Foraminifers 2 Tr
Diatoms   3   –
Radiolarians 1 Tr
Sponge spicules 5 Tr
Silicoflagellates Tr Tr

CARBONATE BOMB (% CaCO₃):
1, 120 cm = 0 |

Sedimentary structure annotations (Core 4): Laminations disturbed by burrows; Dark sand bed with light grains; Scour and fill at base of sand bed (5Y 2/1); Laminations

SITE 566 HOLE CORE 5 CORED INTERVAL 21.9–31.4 m sub-bottom

TIME – ROCK UNIT	BIOSTRATIGRAPHIC ZONE	FOSSIL CHARACTER				SECTION	METERS	GRAPHIC LITHOLOGY	DRILLING DISTURBANCE	SEDIMENTARY STRUCTURES	SAMPLES	LITHOLOGIC DESCRIPTION
		FORAMINIFERS	NANNOFOSSILS	RADIOLARIANS	DIATOMS							
Pleistocene	Pseudoemiliania lacunosa–Emiliania huxleyi					1 2 3 CC	0.5 1.0					Dominant lithology: 0–3.2 m, siliceous mud. Color: dark olive gray (5Y 3/2). Mostly massive and structureless. Some thin laminations and burrows. Scaley fabric present – possibly original feature. Muddy sand beds within this unit.

Minor lithology: 3.2–4.25 m and Core Catcher. Breccia. Color: 7.5YR 3.5/1. Angular serpentine and tuff clasts (up to 3 cm) supported by CaCO₃ rich and dolomite rich matrix (same color). Matrix is variably cemented.

SMEAR SLIDE SUMMARY (%):
1, 125 CC, 5
D M
Texture:
Sand   5   60
Silt   35 30
Clay   60 10
Composition:
Quartz   30 10
Feldspar   2   5
Heavy minerals Tr –
Clay   55 10
Glauconite 1   Tr
Pyrite   2   5
Carbonate unspec. – 70
Calc. nannofossils Tr –
Diatoms   10 –
Radiolarians Tr –
Sponge spicules Tr –

CARBONATE BOMB (% CaCO₃):
2, 60 cm = 12.5
3, 120 cm = 67 |

Sedimentary structure annotations (Core 5): Erosive base; Scaley fabric; Mottling due to burrows (5Y 3.5/2); Burrowing; Scaley fabric; Gradational contact; Void
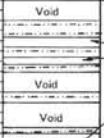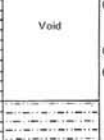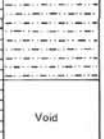
SITE 566 HOLE CORE 6 CORED INTERVAL 31.4–41.1 m sub-bottom

TIME – ROCK UNIT	BIOSTRATIGRAPHIC ZONE	FOSSIL CHARACTER				SECTION	METERS	GRAPHIC LITHOLOGY	DRILLING DISTURBANCE	SEDIMENTARY STRUCTURES	SAMPLES	LITHOLOGIC DESCRIPTION
		FORAMINIFERS	NANNOFOSSILS	RADIOLARIANS	DIATOMS							
						1 CC	0.5 1.0				T	Dominant lithology: serpentinite. Color: N2 5/0.

Refer to thin section form.

Serpentinite with ribbon texture. Younger cross-cutting veins filled with chrysolite. No secondary metamorphic minerals.

Most likely a dunite or hartzburgite that has altered to serpentine under high stress. Chromite shows alteration to Fe₃O₄.

Lots of internal shearing. |

SITE 566 HOLE   CORE 7   CORED INTERVAL 41.1–50.8 m sub-bottom

TIME – ROCK UNIT	BIOSTRATIGRAPHIC ZONE	FOSSIL CHARACTER					SECTION	METERS	GRAPHIC LITHOLOGY	DRILLING DISTURBANCE	SEDIMENTARY STRUCTURES	SAMPLES	LITHOLOGIC DESCRIPTION
		FORAMINIFERS	NANNOFOSSILS	RADIOLARIANS	DIATOMS								
							1	0.5				T	Dominant lithology: serpentinite. Color: light blue green (5BG 6/2) to light blue (5B 7/6).
													Highly sheared perhaps containing a tectonic contact.
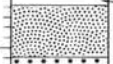
SITE 566 HOLE   CORE 8   CORED INTERVAL 50.8–52.8 m sub-bottom

TIME – ROCK UNIT	BIOSTRATIGRAPHIC ZONE	FOSSIL CHARACTER					SECTION	METERS	GRAPHIC LITHOLOGY	DRILLING DISTURBANCE	SEDIMENTARY STRUCTURES	SAMPLES	LITHOLOGIC DESCRIPTION
		FORAMINIFERS	NANNOFOSSILS	RADIOLARIANS	DIATOMS								
							1	0.5					Dominant lithology: serpentinite. Color: light blue green (5BG 6/2) to light blue (5B 7/6).
													Highly sheared perhaps containing a tectonic contact.

SITE 566 HOLE   CORE 9   CORED INTERVAL 52.8–55.8 m sub-bottom

TIME – ROCK UNIT	BIOSTRATIGRAPHIC ZONE	FOSSIL CHARACTER					SECTION	METERS	GRAPHIC LITHOLOGY	DRILLING DISTURBANCE	SEDIMENTARY STRUCTURES	SAMPLES	LITHOLOGIC DESCRIPTION
		FORAMINIFERS	NANNOFOSSILS	RADIOLARIANS	DIATOMS								
							1	0.5					Dominant lithology: serpentinite. Color: light blue green (5BG 6/2).
							CC	1.0					A lot of mud in this core has probably been derived from the overlying strata.
													Nannofossils derived from the mud are of G. oceanicas zone and are a downhole contaminant.

SITE 566 HOLE A   CORE 1   CORED INTERVAL 0.0–7.0 m sub-bottom

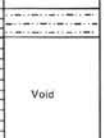| TIME – ROCK UNIT	BIOSTRATIGRAPHIC ZONE	FOSSIL CHARACTER					SECTION	METERS	GRAPHIC LITHOLOGY	DRILLING DISTURBANCE	SEDIMENTARY STRUCTURES	SAMPLES	LITHOLOGIC DESCRIPTION
		FORAMINIFERS	NANNOFOSSILS	RADIOLARIANS	DIATOMS								
late Pliocene	Discoaster brouweri						CC					*	Dominant lithology: only a few fragments of rock were recovered from Core 1 of these there were two main lithologies.

i) Siliceous mud. Color: dark greenish gray (5GY 4/5). Structureless.

ii) Serpentinite. Color: light blue green (5BG 6/2).

SMEAR SLIDE SUMMARY (%):
CC, 12

Texture:
Sand	10
Silt	20
Clay	70
Composition:	
Quartz	1
Feldspar	5
Mica	1
Clay	65
Pyrite	2
Carbonate unspec.	15
Calc. nannofossils	Tr
Diatoms	5
Radiolarians	2
Sponge spicules	3
Silicoflagellates	1

SITE 566   HOLE C   CORE H1   CORED INTERVAL   0.0–49.8 m sub-bottom

TIME – ROCK UNIT	BIOSTRATIGRAPHIC ZONE	FOSSIL CHARACTER					SECTION	METERS	GRAPHIC LITHOLOGY	DRILLING DISTURBANCE	SEDIMENTARY STRUCTURES	SAMPLES	LITHOLOGIC DESCRIPTION
		FORAMINIFERS	NANNOFOSSILS	RADIOLARIANS	DIATOMS								

late Miocene — *Discoaster quinqueramus*

Void
0.5 — 1
1.0
Void
Void
— Voids

2

Void

3

4 — Void

5 — Void

Void

CC — ← Possible ash band (very dark gray – 5Y3 5/1)

Dominant lithology: massive mud. Color: dark olive gray (5Y 5/2). Very soupy structureless sediment. Lots of drilling disturbance.

Site 566C, Core 1, 49.8–59.3 m sub-bottom: no recovery.

SITE 566   HOLE C   CORE 2   CORED INTERVAL   59.3–68.8 m sub-bottom

TIME – ROCK UNIT	BIOSTRATIGRAPHIC ZONE	FOSSIL CHARACTER					SECTION	METERS	GRAPHIC LITHOLOGY	DRILLING DISTURBANCE	SEDIMENTARY STRUCTURES	SAMPLES	LITHOLOGIC DESCRIPTION
		FORAMINIFERS	NANNOFOSSILS	RADIOLARIANS	DIATOMS								

late Miocene — *Discoaster quinqueramus*

1 — 0.5

Void
— Black pumice clasts

Dominant lithology: sand (8–58 cm). Color: dark olive gray (5Y 3/2). Structureless sand grades down into the gravel below -- this grading is probably a drilling phenomena. "Ashy sand".

Minor lithologies:
i) Gravel (57–65 cm). Color: black (5Y 2/2) to olive gray (5Y 4/2). Angular clasts of mudstone and pumice up to 2 cm diameter. Clast supported and poorly sorted.

ii) Mud (65–84 cm). Color: dark olive gray (5Y 3/2) structureless.

SMEAR SLIDE SUMMARY (%):

	1, 26	1, 64
Texture:		
Sand	90	20
Silt	10	30
Clay	–	50
Composition:		
Quartz	70	30
Feldspar	20	10
Heavy minerals	5	3
Clay	–	50
Volcanic glass	3	–
Glauconite	Tr	2
Pyrite	2	1
Foraminifers	Tr	–
Calc. nannofossils	Tr	Tr
Diatoms	Tr	–
Radiolarians	Tr	Tr

SITE 566 HOLE C CORE 3 CORED INTERVAL 68.8–78.5 m sub-bottom

TIME – ROCK UNIT	BIOSTRATIGRAPHIC ZONE	FOSSIL CHARACTER				SECTION	METERS	GRAPHIC LITHOLOGY	DRILLING DISTURBANCE	SEDIMENTARY STRUCTURES	SAMPLES	LITHOLOGIC DESCRIPTION
		FORAMINIFERS	NANNOFOSSILS	RADIOLARIANS	DIATOMS							
late Miocene	Discoaster quinqueramus					CC			□		* *	Dominant lithology: mud. Color: dark olive gray (5Y 3/2). Only one 13 cm sample in the Core Catcher structure.

Minor lithology:
i) Small angular clasts of tuff – up to 2 cm in diameter.

ii) Small angular clasts of calcareous mud – up to 2 cm in diameter.

SMEAR SLIDE SUMMARY (%):
                              CC, 1 CC, 8

Texture:
Sand   66   30
Silt   34   20
Clay   –   50
Composition:
Quartz   20   35
Feldspar   35   10
Heavy minerals   2   3
Clay   –   45
Glauconite   –   2
Pyrite   1   2
Carbonate unspec.   40   3
Calc. nannofossils   Tr   Tr
Diatoms   Tr   Tr
Radiolarians   Tr   –

Site 566C, Core 4, 78.5–88.1 m sub-bottom: no recovery.

SITE 566 HOLE C CORE H2 CORED INTERVAL 88.1–109.1 m sub-bottom

TIME – ROCK UNIT	BIOSTRATIGRAPHIC ZONE	FOSSIL CHARACTER				SECTION	METERS	GRAPHIC LITHOLOGY	DRILLING DISTURBANCE	SEDIMENTARY STRUCTURES	SAMPLES	LITHOLOGIC DESCRIPTION
		FORAMINIFERS	NANNOFOSSILS	RADIOLARIANS	DIATOMS							
late Miocene						1	0.5 1.0		□ □ □		* *	Structureless drilling breccia comprising two dominant lithologies.
						2			□			
						CC					*	

Mudstone. Color: dark olive gray (5Y3 5/2). Structureless.

Sandstone. Color: dark greenish gray (5GY 4/2). Lithified sandstone, matrix rich in $CaCO_3$. Sand- to gravel-sized grains. High percentage of volcanic rock fragments – angular. No internal sedimentary structures.

SMEAR SLIDE SUMMARY (%):
                         1, 20 1, 90 CC, 1
                         D   D   D
Texture:
Sand   60   5   75
Silt   20   10   15
Clay   20   85   10
Composition:
Quartz   20   5   5
Feldspar   30   2   25
Mica   –   –   1
Heavy minerals   5   Tr   4
Clay   20   80   –
Volcanic glass   –   Tr   –
Palagonite   –   Tr   –
Glauconite   1   –   –
Pyrite   10   10   2
Carbonate unspec.   10   –   20
Calc. nannofossils   Tr   Tr   –
Radiolarians   Tr   Tr   –
Sponge spicules   Tr   Tr   –
Silicoflagellates   –   Tr   –
Volcanic fragments   –   –   33

SITE 566 HOLE C CORE 5 CORED INTERVAL 109.1–117.2 m sub-bottom

TIME – ROCK UNIT	BIOSTRATIGRAPHIC ZONE	FOSSIL CHARACTER				SECTION	METERS	GRAPHIC LITHOLOGY	DRILLING DISTURBANCE	SEDIMENTARY STRUCTURES	SAMPLES	LITHOLOGIC DESCRIPTION
		FORAMINIFERS	NANNOFOSSILS	RADIOLARIANS	DIATOMS							

Dominant lithology: serpentinite and remnants of serpentinized peridotite. Color: dusky blue (5BP 3/2).

See igneous rock core description.

This core has been highly disturbed by drilling. The serpentinite has weathered to a clay — some original structures visible. Intact, unweathered blocks of peridotite found throughout the core.

SITE 566 HOLE C CORE 6 CORED INTERVAL 117.2–126.9 m sub-bottom

TIME – ROCK UNIT	BIOSTRATIGRAPHIC ZONE	FOSSIL CHARACTER				SECTION	METERS	GRAPHIC LITHOLOGY	DRILLING DISTURBANCE	SEDIMENTARY STRUCTURES	SAMPLES	LITHOLOGIC DESCRIPTION
		FORAMINIFERS	NANNOFOSSILS	RADIOLARIANS	DIATOMS							

← Talc layer

Dominant lithology: serpentinite. Color: black (N2/0).

Large broken pieces of serpentinite. Altered rims along fractures. Altered pyroxene crystals visible < 5%. Black magnetite or chromite crystals <7%.
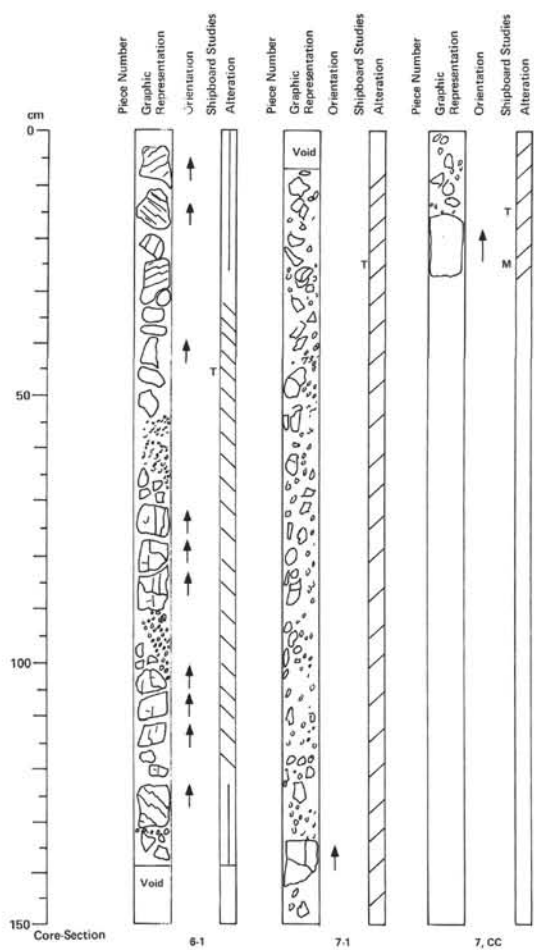
See thin section description.

SITE 566 HOLE C CORE 7 CORED INTERVAL 126.9–136.6 m sub-bottom

TIME – ROCK UNIT	BIOSTRATIGRAPHIC ZONE	FOSSIL CHARACTER				SECTION	METERS	GRAPHIC LITHOLOGY	DRILLING DISTURBANCE	SEDIMENTARY STRUCTURES	SAMPLES	LITHOLOGIC DESCRIPTION
		FORAMINIFERS	NANNOFOSSILS	RADIOLARIANS	DIATOMS							

Dominant lithology: serpentinite. Color: Black (N2/0). Some lighter bluish gray (5B 4/1) altered rims. Highly fractured.

Pyroxene crystals < 10%. Magnetite/chromite <10%.

See thin section description.

cm

Piece Number	Graphic Representation	Orientation	Shipboard Studies	Alteration	Piece Number	Graphic Representation	Orientation	Shipboard Studies	Alteration	Piece Number	Graphic Representation	Orientation	Shipboard Studies	Alteration

Core-Section   6-1   7-1   7, CC

84-566C-6-1   Depth: 379.2–380.1 m

Dominant lithology: black (N2/0) serpentinite containing pyroxene (<10%) and magnetite/chromite (<10%). Highly fractured and sheared. Serpentinite drilling breccia at 57–70, 90–103, and 128–133 cm.

Thin section: serpentinite — originally peridotite? — fibrous to granular coarse texture. Pyroxene + olivine to serpentinite 74%? to other opaques 25%.

84-566C-7-1   Depth: 3801.9–3811.6 m

Dominant lithology: serpentinite. Color: black (N2/0). Moderately altered; pieces shattered by drilling. Some lighter bluish gray (5B 4/1) altered rims along fractures in bigger, broken pieces. There are pyroxene crystals about 0.5–2 mm <5% and black (magnetite/chromite) <7%.

84-566C-7, CC   Depth: 3801.9–3811.6 m

Dominant lithology: massive black serpentinite (N2/0) containing pyroxene (<10%) crystals up to 2 mm and magnetite or chromite (<10%) crystals up to 0.5 mm. Bluish-gray weathered rims on fractured surfaces. Mostly shattered into drilling breccia.